University of Stavanger

Faculty of Science and Technology

MASTER'S THESIS

Study program/Specialization: Petroleum Geosciences Engineering	Spring semester, 2015 Open
Writer: Ayyub Aghamoghlanov	_____ (Writer's signature)
Faculty supervisor: Rodmar Ravnas External supervisor(s): Lothar Schulte	
Title of thesis: Influence of different modeling techniques on reservoir volume	
Credits (ECTS): 30	
Keywords: **Sequential Indicator Simulation** **Object modeling** **Acoustic impedance cube** **Reservoir volume spread** **Reservoir polygons**	Pages: 78 + Front page: 12 + CD Stavanger, June 15, 2015

.

Copyright

by

Ayyub Aghamoghlanov

2015

Influence of different modeling techniques on reservoir volume

by

Ayyub Aghamoghlanov

Master Thesis

Presented to the Faculty of Science and Technology

The University of Stavanger

The University of Stavanger

June, 2015

Acknowledgements

I would like to express my very great appreciation to Lothar Schulte for his valuable and suggestions during this research work. His willingness to give his time so generously has been very much constructive appreciated. I would like to express my gratitude to Pr. Rodmar Ravnas, for his patient guidance, enthusiastic encouragement and useful critiques of this research work. I'm also very thankful to Alejandro Escalona for offering me a working place in his own computer lab, which is provided with licensed version of Petrel 2013.

Finally, I wish to thank my parents for their support and encouragement throughout my study at University of Stavanger.

Abstract

Influence of different modeling techniques on reservoir volume

Ayyub Aghamoghlanov

The University of Stavanger, 2015

Supervisors: Lothar Schulte, Rodmar Ravnas

Facies modeling is one of the initial stages on the way to reservoir volume calculations. Typically, for each depositional environment a particular facies modeling method is used. The geology of the area of investigation can be described, by a stacked channel (deltaic) depositional environment. This work represents a set of models, which are created using Object Modeling and Sequential Indicator Simulation method. Each facies modeling method has its own parameters, which are influencing the reservoir volume. Sequential Indicator Simulation is a pixel based modeling method, which is based on an estimation of the probability of each facies at every grid point. The facies at the grid point is derived from the cumulative distribution function (CDF) of the facies probabilities and a random number generator used for deriving the facies from the (CDF). The main modeling parameters of the Sequential Indicator Simulation method are: The Global seed number, which is controlling the random number generator, the Major, Minor and Vertical variogram range. In the Object based modeling method, the main parameters describing channel geometry are: Thickness, Width, Amplitude and Wavelength.

One of the main purposes of this project is to investigate the influence of the modeling parameters on the reservoir volume spread. Research is also covering the influence of the well positions with respect to the upscaled well, on the reservoir volume spread. This is accomplished thru defining areas of investigations at different locations with respect to the one upscaled well.
Another topic of the thesis is the study of the influence of the “Global facies fraction” on the reservoir volume.

Finally, a close look is taken on the seismic impedance as a guide for facies modeling, which can help reducing the reservoir volume uncertainty. The outcome of the study will be a set of recommendations for facies modeling of a stacked channel environment that result in a more reliable reservoir volume estimation and uncertainty evaluation.

Table of Contents

Table of Contents viii

List of Tables ix

List of Figures xi

CHAPTER 1 : INTRODUCTION **1**

1.1 Objectives 2

1.2 Dataset 4

1.3 Methodology 5

1.3.1 Sequential Indicator Simulation modeling method 5

1.3.2 Object modeling method 12

1.3.3 Influence of Sequential Indicator Simulation modeling parameters on reservoir volume distribution 18

1.3.4 Influence of Object modeling method parameters on reservoir volume distribution 22

1.3.5 The Seismic Acoustic impedance cube 25

CHAPTER 2 : OBSERVATIONS **28**

2.1 Sequential Indicator Simulation modeling method 28

2.2 Object modeling method 39

2.3 Acoustic Impedance cube 46

CHAPTER 3 : DISCUSSION **55**

3.1 Sequential Indicator Simulation method 55

3.2 Object modeling method 55

3.3 Reservoir size impact on reservoir volume spread 56

3.4 Variation of the volume spread distribution in polygons with respect to the upscaled well 56

3.5 Influence of Acoustic Impedance cube on reservoir volume spread 58

3.6 Reservoir volume P50 stability, along with P10 and P90 values 59

3.7 Volume spread analysis for Sequential Indicator Simulation and

Object modeling methods 59

CHAPTER 4 : CONCLUSIONS 62

REFERENCES 64

List of Tables

Table 1: Range of modeling parameters according to the graph produced by Leeder (1973)..... 13

Table 2: Sequential Indicator Simulation: volume spreads for polygon 3, with radius 500m. 30

Table 3: Sequential Indicator Simulation: volume spread for polygon 3, with radius 1000m 30

Table 4: Sequential Indicator Simulation: volume spread function for the polygons 1, 2 and 3 with radius 500m. 31

Table 5: Sequential Indicator Simulation volume spread for polygon 3, with radius 500m and 1000m. 33

Table 6: Sequential Indicator Simulation volume spread for polygon 3, using "Major range = Minor range", and vertical ranges: 1m, 10m and 50m. 35

Table 7: Sequential Indicator Simulation volume spread for polygon 3, using "Minor range = 70%Major range", and vertical ranges: 1m, 10m and 50m. 35

Table 8: Sequential Indicator Simulation: volume spreads for polygon 3 with radius 500m using different horizontal ranges…….....37

Table 9: Sequential Indicator Simulation: volume spread for polygon 3 with radius 1000m, using different horizontal ranges..... 37

Table 10: Channel thickness variations 39

Table 11: Volume spread distribution for three polygons obtained by channel thickness variations..... 39

Table 12: Channel width variations 41

Table 13: Volume spread distribution for three polygons obtained by channel width variations..... 41

Table 14: Channel amplitude variations 41

Table 15: Volume spread distribution for three polygons obtained by channel amplitude variations..... 44

Table 16: Channel wavelength variations..... 44

Table 17: Volume spread distribution for three polygons obtained by channel wavelength variations..... 44

Table 18: Volume spread based on Sequential Indicator Simulation guided by the Acoustic impedance volume for Polygon 1 and Polygon 3 52

Table 19: Volume spread based on Sequential Indicator Simulation for Polygon 1 and Polygon 3 52

List of Figures

Figure 1: Sequential Indicator Simulation method. Major and Minor variogram ranges are same 2

Figure 2: Sequential Indicator Simulation method. Minor is smaller than Major range 3

Figure 3: Object modeling method 3

Figure 4: Simple conceptual model 4

Figure 5: Well data 4

Figure 6: Map showing sand probability at well location and calculated sand probability at grid points using kriging 6

Figure 7: Variogram scheme 6

Figure 8: Cumulative Distribution function plot with random number 7

Figure 9: Object modeling method 9

Figure 10: Sequential Indicator Simulation method. Major and Minor anisotropy ranges: 700 9

Figure 11: Sequential Indicator Simulation method. Major and Minor anisotropy ranges: 1000 10

Figure 12: Sequential Indicator Simulation method. Major and Minor range: 5000. Seed: 1 11

Figure 13: Sequential Indicator Simulation method. Major and Minor range: 5000. Seed: 50 11

Figure 14: Map view description of channel parameters 12

Figure 15: Cross-section of the channelized model 12

Figure 16: Cross section of the channelized model. Channel thickness 10m 13

Figure 17: Cross section of the channelized model. Channel thickness 70m 13

Figure 18: Channel width 60m 14

Figure 19: Channel width 960m 14

Figure 20: Channel amplitude 110m 15

Figure 21: Channel amplitude 610m 15

Figure 22: Channel wavelength 400m..... 16

Figure 23: Channel wavelength 10400m..... 16

Figure 24: Object modeling method. Seed number 1..... 17

Figure 25: Object modeling method. Seed number 10..... 17

Figure 26: Conceptual model with reservoir and non-reservoir facies. Location of three circular reservoir polygons 19

Figure 27: Sequential Indicator Simulation method workflow 20

Figure 28: Reservoir volume distribution CDF (Cumulative Distribution Function) graph ... 21

Figure 29: Object modeling method workflow 22

Figure 30: (Leeder, 1973) published data from modern high sinuosity rivers (>1.7) on the relationship between Channel Depth and Channel Width..... 23

Figure 31: Data published by (Leopold and Wolman, 1960) and (Carlston, 1965). The ratio of meander belt width (Meander amplitude) vs channel width. 24

Figure 32: Data published by (Wonham et al., 2000). The ratio of channel width vs meander wavelength 25

Figure 33: The Seismic acoustic impedance cube..... 26

Figure 34: Reservoir facies probability distribution, according to acoustic impedance responses..... 27

Figure 35: Location of reservoir polygon 3..... 28

Figure 36: a) Reservoir volume spread distributions for polygon with radius 500m using different vertical ranges. b) Reservoir volume spread distributions for polygon with radius 1000musing different vertical ranges..... 29

Figure 37: a) Reservoir volume spread distributions for different polygons with radius 500m. b) Sequential Indicator Simulation model of reservoir facies, with the position of the reservoir polygons..... 32

Figure 38: Reservoir volume distribution graphs for polygon 3 with radius 500m and 1000m..... 34

Figure 39: a) Reservoir volume spread distributions for polygon 3 with radius 500m using equal horizontal ranges. b) Reservoir volume spread distributions for polygon 3 with radius 1000m using different horizontal ranges 36

Figure 40: a) Reservoir volume spread distributions for polygon 3 with radius 500m using equal and different horizontal anisotropy ranges. b) Reservoir volume spread distributions for polygon 3 with radius 1000m using equal and different horizontal anisotropy ranges. 38

Figure 41: a) Volume spread distributions for three polygons with radius 500m, obtained by increasing the channel thickness. b) Volume spread distributions for three polygons with radius 1000m, obtained by increasing the channel thickness..... 40

Figure 42: a) Volume spread distributions for three polygons with radius 500m, obtained by increasing the channel width. b) Volume spread distributions for three polygons with radius 1000m, obtained by increasing the channel width 42

Figure 43: a) Volume spread distributions for three polygons with radius 500m, obtained by increasing the channel amplitude. b) Volume spread distributions for three polygons with radius 1000m, obtained by increasing the channel amplitude..... 43

Figure 44: a) Volume spread distributions for three polygons with radius 500m, obtained by increasing the channel wavelength. b) Volume spread distributions for three polygons with radius 1000m, obtained by increasing the channel wavelength 45

Figure 45: The seismic acoustic impedance cube applied on the model..... 46

Figure 46: Reservoir facies probability distribution, according to acoustic impedance responses..... 47

Figure 47: Non-Reservoir facies probability distribution, according to acoustic impedance responses..... 48

Figure 48: Reservoir (sand) facies probability cube..... 49

Figure 49: Non-reservoir (shale) facies probability cube..... 50

Figure 50: a) Reservoir volume spread distributions for Acoustic impedance in polygon 3 with radius 500m, using different vertical ranges b) Reservoir volume spread distributions for Sequential Indicator Simulation in polygon 3 with radius 500m, using different vertical ranges 51

Figure 51: a) Reservoir volume spread distributions for polygon 1 with radius 500m using equal horizontal anisotropy ranges. b) Reservoir volume spread distributions for polygon 3 with radius 500m using equal horizontal anisotropy ranges 53

Figure 52: a) Reservoir volume distribution for polygon 1 with radius 500m, obtained using Seismic acoustic impedance cube. b) Reservoir volume distributions for polygon 1 with radius 500m using Sequential Indicator Simulation method..... 54

Figure 53: a) Channel distributions in Object modeling method. Seed number 10
b) Channel distributions in Object modeling. Seed number 50..... 57

Figure 54: a) Sand probability of the model based on Acoustic impedance
b) Sand probability of the model based on Sequential Indicator Simulation 58

Figure 55: Reservoir volume distribution of the channels, obtained via channel width variations. Stability of P50 value among P10 and P90 59

Figure 56: Sequential Indicator Simulation method. Reservoir volume spread distributions for different polygons with radius 500m. Vertical range is taken 10m.. 60

Figure 57: Object modeling method. Reservoir volume spread distributions for different polygons with radius 500m. 60

Figure 58: Reservoir facies (sand facies) thickness map for one Sequential Indicator Simulation. Major and Minor ranges are equal (700). Vertical range is 50.. 61

Figure 59: Reservoir facies (sand facies) thickness map for one Object Modelling method. Channel width is 960m. 61

Chapter 1: INTRODUCTION

Facies model building is typically done by either one of the following methods: pixel based Sequential Indicator Simulation (Figure 1) or Object based modeling (Figure 2). The choice for the most appropriate method depends upon the available information, the characteristics and the geological knowledge about the field. The input data for both methods is subdivided into: hard data (e.g. wells data, such as facies proportions), and soft data (e.g. seismic attribute cubes). As a result, each of these methods comes up with a distinct architecture and facies distribution.

Reservoir models which are created using Sequential Indicator Simulation are represented by sand patches whose size is controlled by the horizontal model variogram range (Figure 1). Sand patches can also be elongated in a user defined direction in order to capture the facies anisotropy that is given by the channels. This is accomplished thru working with two horizontal variogram ranges of different sizes that are perpendicular to each other as shown in Figure 3.

Reservoir models based on Object modeling consist of objects, such as channels or simple geometrical bodies, which are characterized by specific porosity and permeability ranges, while the background shale has low porosity and permeability values. All modeling methods described above will be applied to a conceptual structural model. This study intends to describe the variation of the reservoir volume, with respect to the changes of the variogram parameters of Sequential Indicator Simulation, as well as, the variations of the geometrical parameters used in channel (Object) modeling.

The reservoir volumes are derived for circular polygons, which are located in different areas, relatively to the wells. In this way the influence of the wells on the reservoir volume uncertainty can be analyzed.

In addition, the possible influence of the size of the area given by the circular polygon on the reservoir volume distribution will be investigated.
Finally, this project analyzes how the seismic impedance cube can influence reservoir volume distribution.

In this study we will use data from 6 wells. Interpretation and analysis are aimed to fulfill the objectives stated below:

1.1 Objectives:

- Understanding the influence of the different facies modeling parameters on the modeled reservoir volume and reservoir volume uncertainty
- Investigation of advantages and disadvantages of Sequential Indicator Simulation and Object modeling, and their impact on reservoir volume.
- Volume spread analysis. P50 stability, comparing to P10 and P90
- Analysis of changes in volume spread, in reservoirs, located differently with respect to the well DW1 .
- Analysis of the influence of the seismic impedance cube, used for facies modeling on reservoir volume uncertainty.
- The usage of analogue data to limit the parameter uncertainty of the facies modeling.

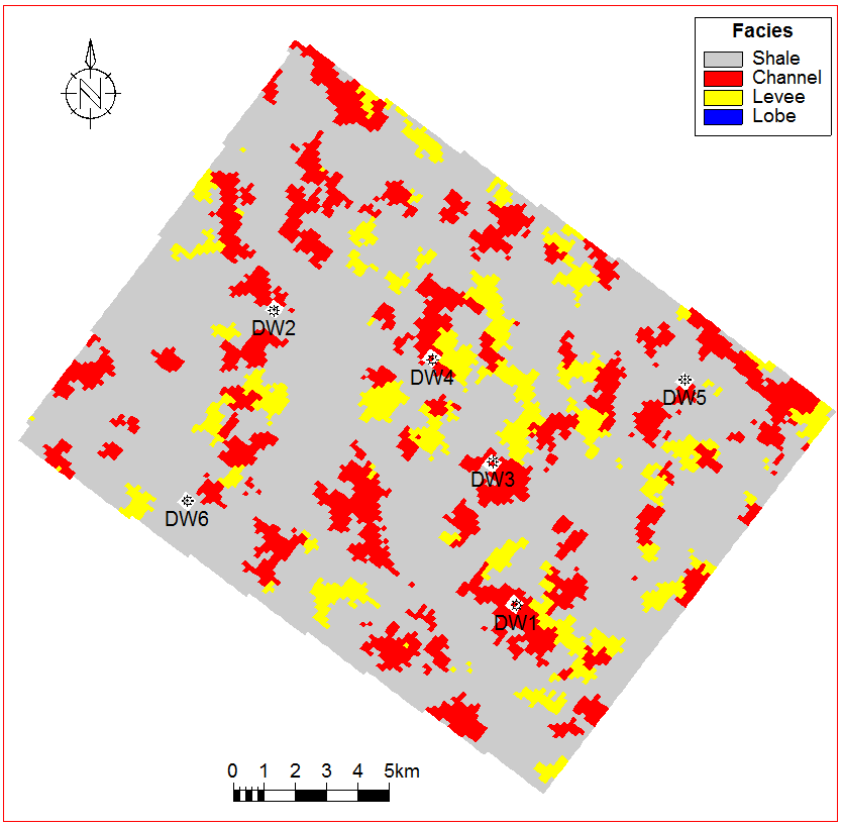

Figure 1: Sequential Indicator Simulation method. Major and Minor variogram ranges are same

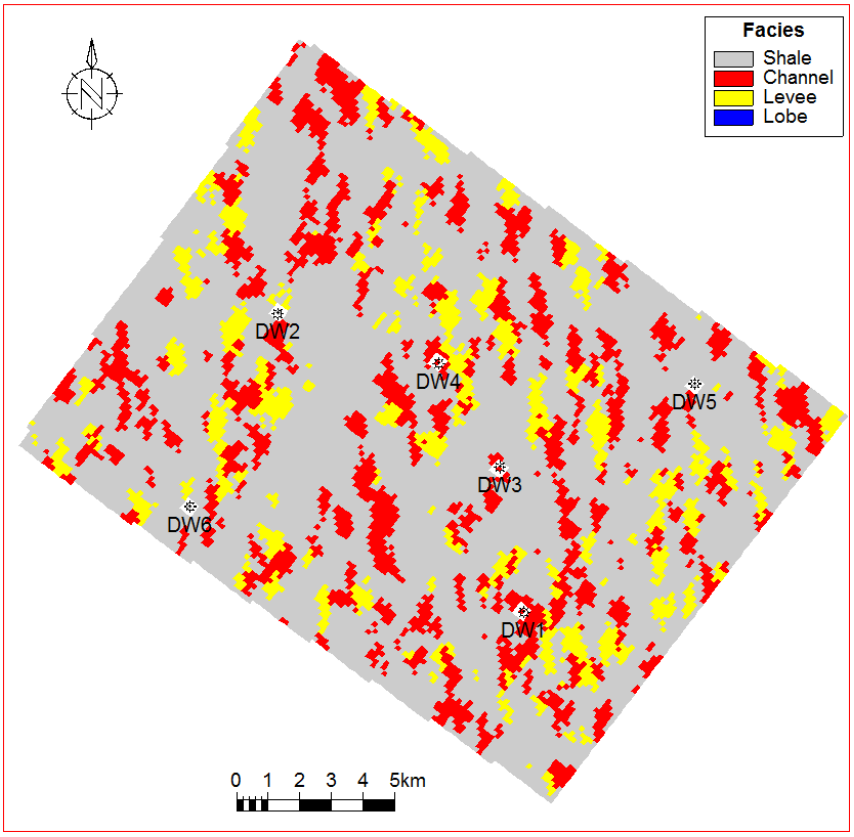

Figure 2: Sequential Indicator Simulation method. Minor is smaller than Major range.

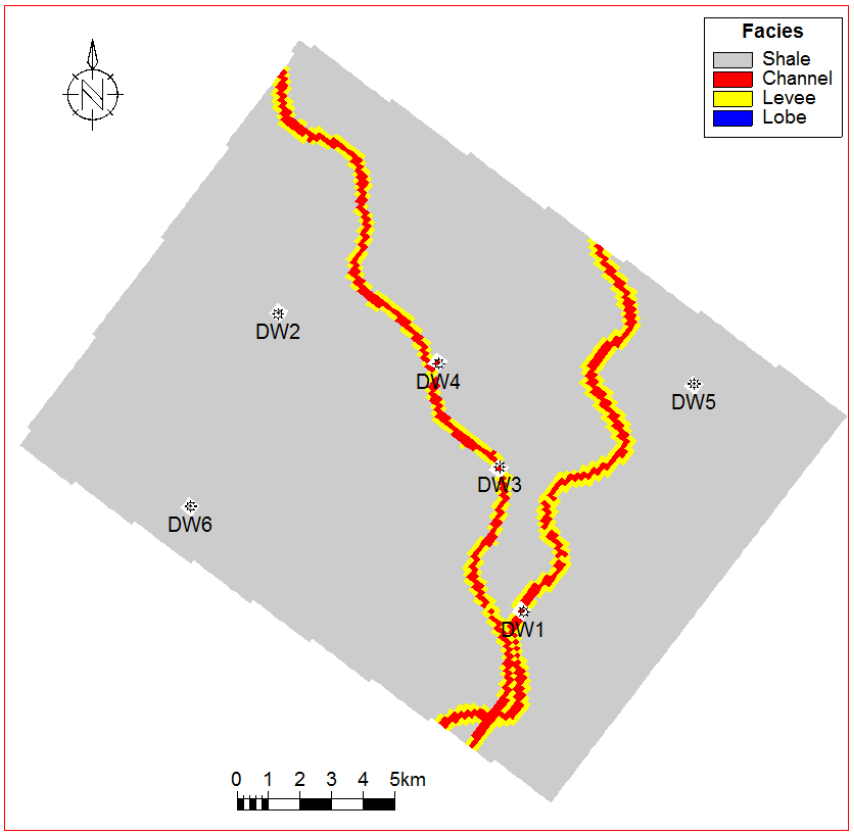

Figure 3: Object modeling method

1.2 Dataset

Dataset used for research in this project includes:

- Simple rectangular structural model of dimensions 15000m by 16000m (Figure 4)
- Six wells with porosity, permeability and gamma ray logs: DW6. DW1, DW2, DW4, DW5 and DW3
- Seismic impedance cube

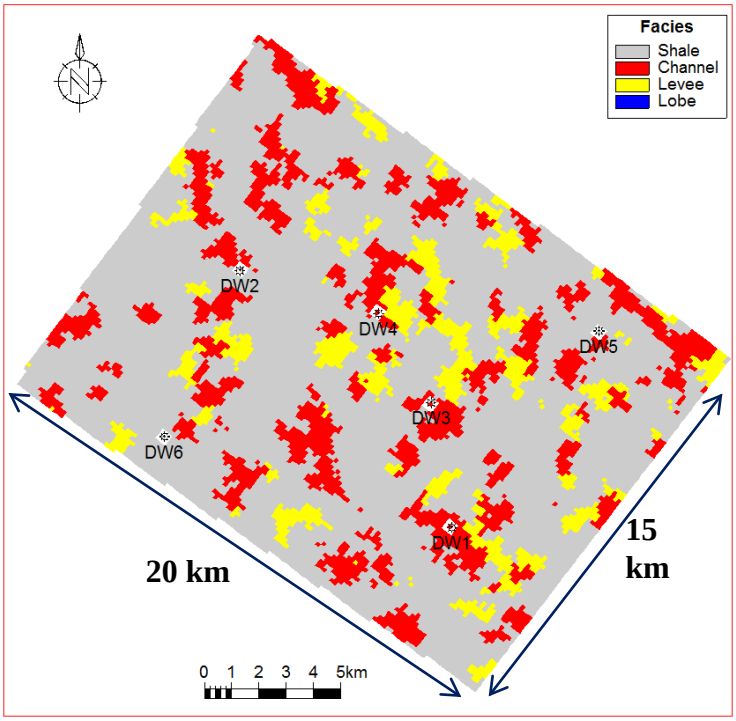

Figure 4: Simple conceptual model

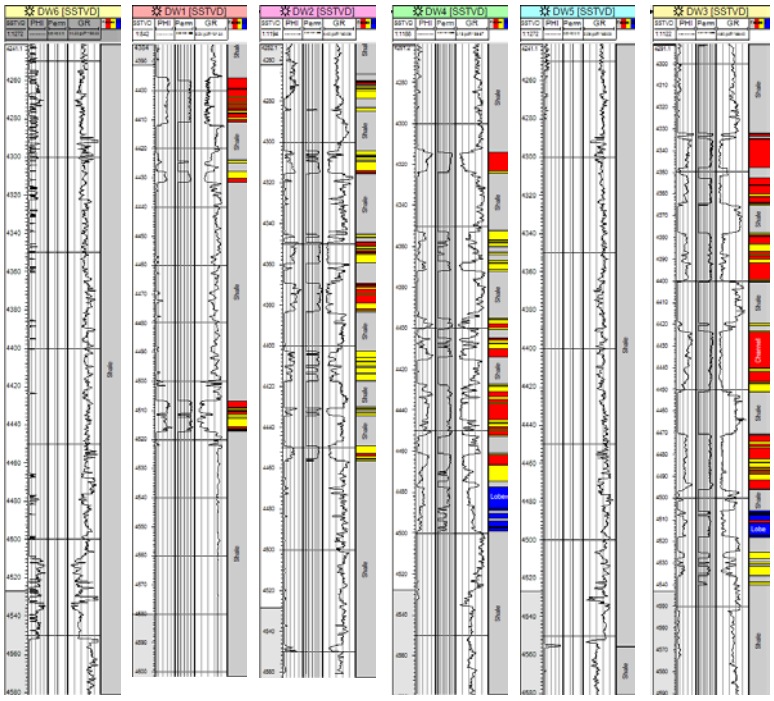

Figure 5: Well data

1.3 Methodology

The main goal of this project is to assess the influence of the major parameters of two facies modeling methods on the reservoir volume uncertainty: Sequential Indicator Simulation method and Object Modeling method. Each facies modeling parameter has its own influence on reservoir volume spread, and the best way to investigate this, is to create different models, by changing one parameter at a time.

1.3.1 Sequential Indicator Simulation

Sequential Indicator Simulation is a facies modeling method, which relates to Pixel-based reservoir modeling technique. In many cases, Pixel-based reservoir modelling can approximate the reservoir in terms of its sedimentological architecture if sufficiently wells are available. Sequential Indicator Simulation is a geostatistical method that addresses the uncertainties, caused by, lack of data between the wells (Seifert and Jensen, 1999).

The way Sequential Indicator Simulation works is discussed in the following: at the wells the facies which is going to be modeled is given a probability of "1", if it is encountered at the well and "0" if it is not. Figure 6 shows the probability of sand at well locations, marked by , if the well shows sand (probability "1") and by , if the well does not show sand (sand probability equal "0"). Grid points with calculated sand probability are represented by . These values are interpolated in order to get the probability of encountering sand at grid point . The method used for calculating the facies probability at the grid point , is called "Simple Kriging".

Simple kriging, is an interpolation technique that takes fundamental statistical properties of the data (mean and variance) into account. Kriging is using a variogram model that needs to be derived from the sample variogram of the data (Caers, 2005).

Variograms are used to describe the variance of data pairs of a separation distance called lag (Caers, 2005) (Figure 7). Data pairs showing a large lag typically show a large variance, meaning their values show a large difference. Typically the variance of the data pairs decreases with smaller lags. The *Range* describes the distance between data pairs beyond which the variance is varying around a constant high value, the *Sill*. Beyond this range the data pairs do not show any correlation. A *Nugget* means that data pairs that are very close to each other or share the same location (zero lag) show different values

(Caers, 2005). Such a behavior could be attributed to noise. For this project, the variogram analysis of the data is not needed, because the goal is to understand the influence of the horizontal and vertical variogram range (anisotropy ranges) on the volume uncertainty

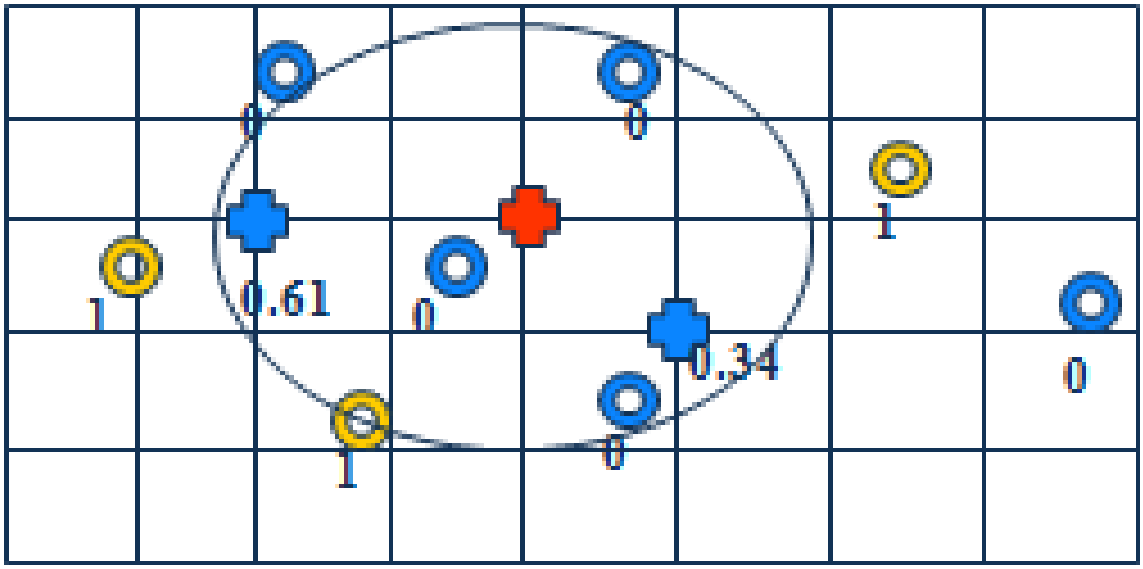

Figure 6: Map showing sand probability at well location and calculated sand probability at grid points using kriging.

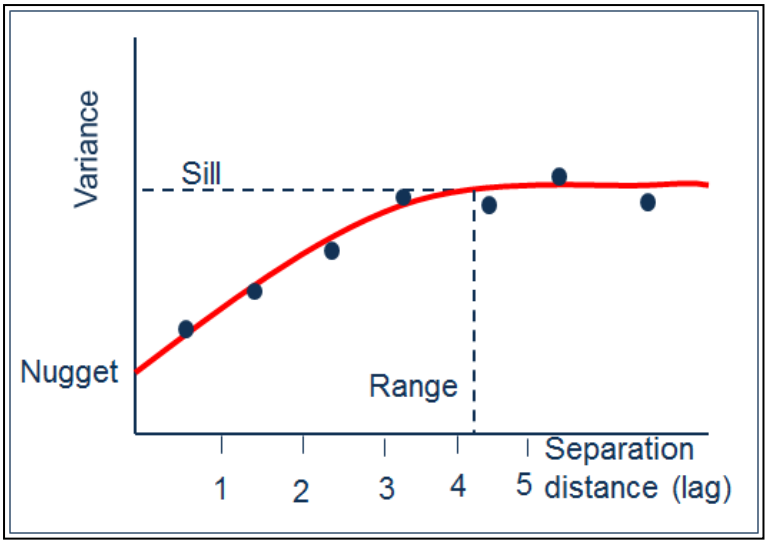

Figure 7: Variogram scheme.

The two horizontal ranges are measured in perpendicular directions. When they are of the same size the data is regarded as isotropic, in case of a difference between the two ranges the data is anisotropic.

When the facies probability has been derived the Cumulative Distributive Function (CDF) is set up from the facies probabilities, as shown in Figure 8. A random number between 0 and 1 is drawn via a random number generator that is controlled by the so-called "*Seed*" number in the used modeling software package *Petrel* (Figure 8). Outside the radius of influence of the data points defined by the variogram range Simple kriging provides the mean value given by all data. In the case of indicator simulation this mean value is defined by the facies fraction given by the wells. This so-called "*Global fraction"* influences increasingly the cumulative distribution function of grid cells with increasing distance from the wells. It is the "*Global distribution"* that defines the facies fraction of the model to a large degree.

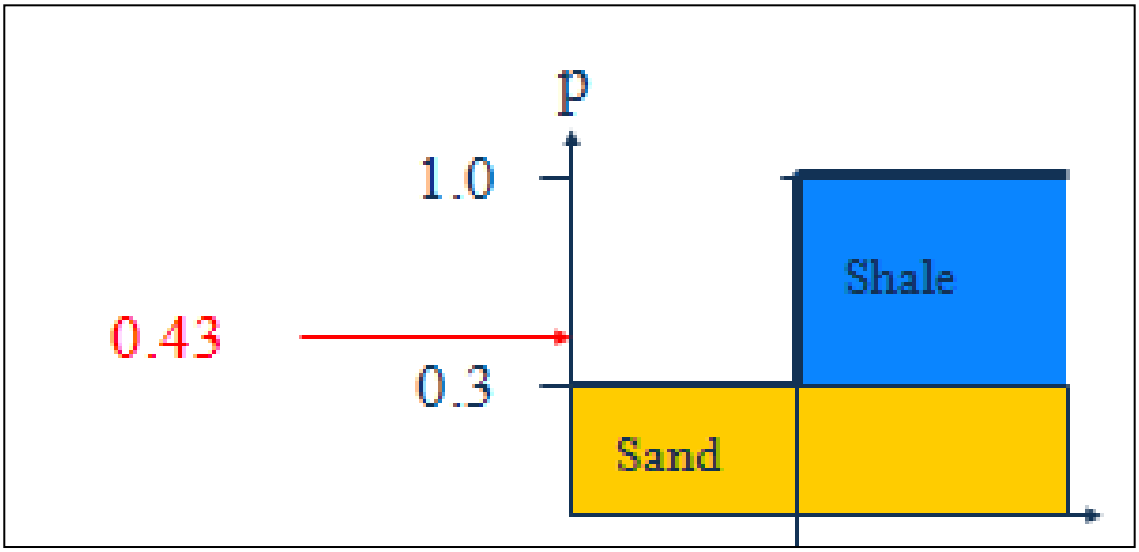

Figure 8: Cumulative Distribution Function plot with random number

As shown in Figure 9, small ranges applied to the Sequential Indicator Simulation method, give a lot of small sand patches spread all over the model. In Figure 10 the major and minor ranges have the same large value, and as a result deliver a few big sand patches. The relationship between the small and the large horizontal range define the elongation of the facies patches (Figure 10).

The operation mechanism of Seed number on Sequential Indicator Simulation method is visually explained in Figure 12 and Figure 13. In Figure 12 and Figure 13 are shown two models with the same variogram ranges, but with different Seed numbers. Therefore, the global facies fraction distribution is the same for both models in Figure 12 and Figure 13. As it can be seen, the patches of channel sand, levee and shale are distributed differently in the model with Seed number 1 and Seed number 50. It is the Seed that is controlling the distribution of the facies patches.

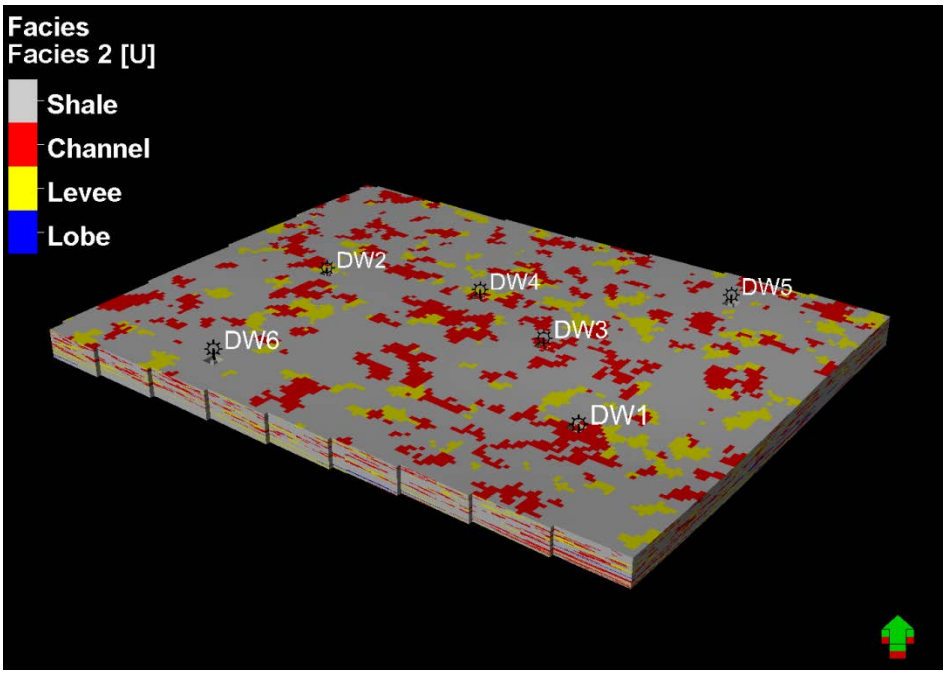

Figure 9: Sequential Indicator Simulation method. Major and Minor anisotropy ranges: 700

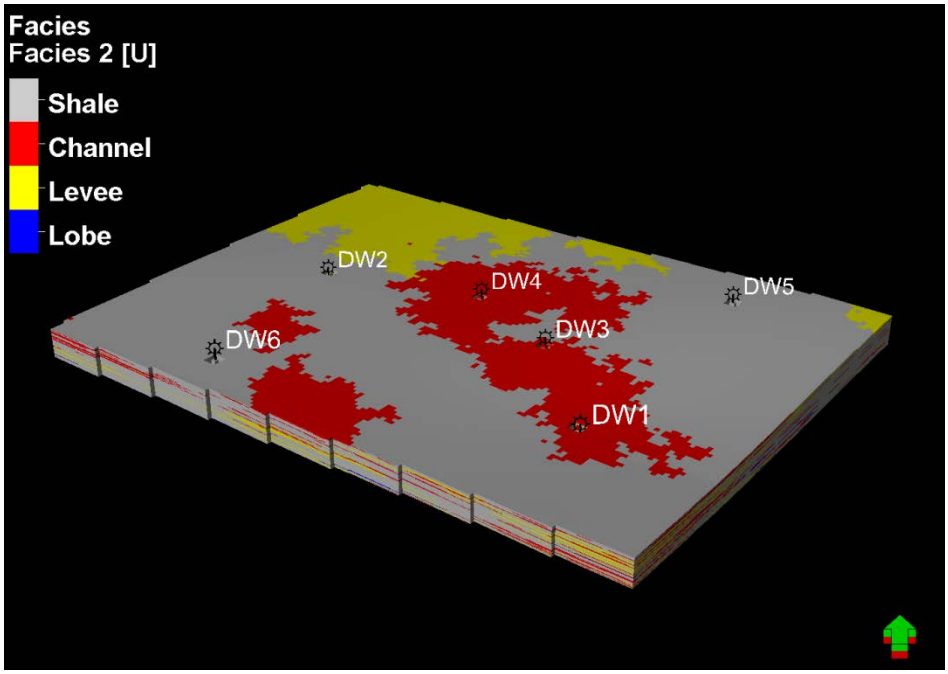

Figure 10: Sequential Indicator Simulation method. Major and Minor anisotropy ranges: 5000

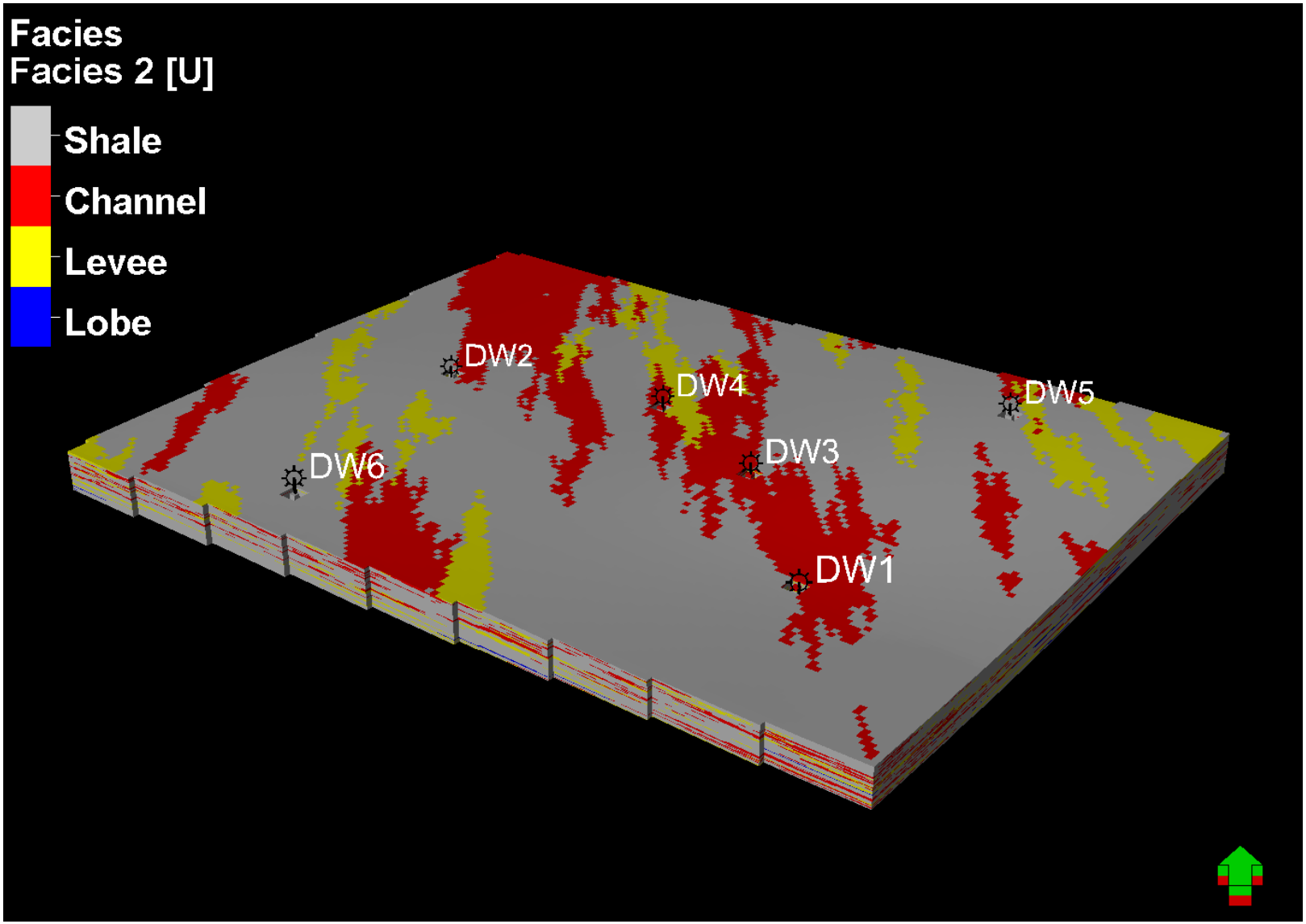

Figure 11: Sequential Indicator Simulation Method. Major range: 5000, Minor range: 1000

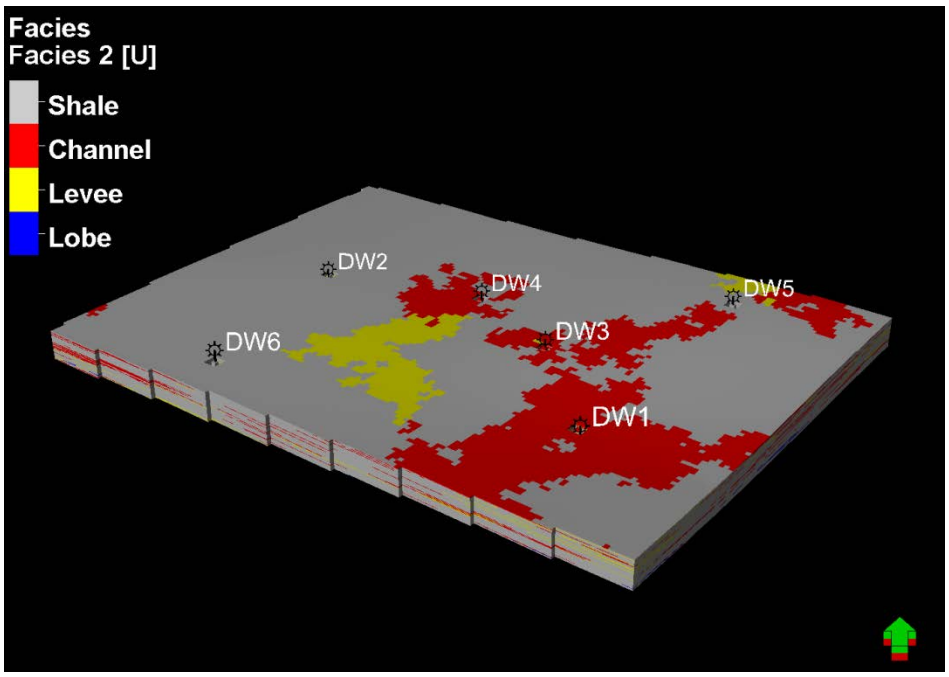

Figure 12: Sequential Indicator Simulation method. Major and Minor range: 5000. Seed: 1

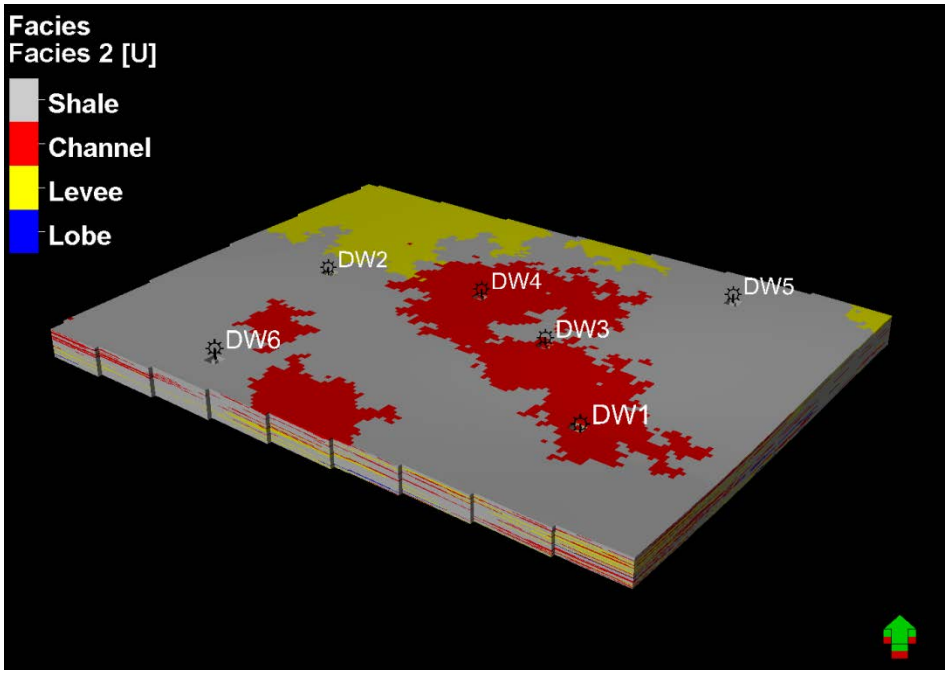

Figure 13: Sequential Indicator Simulation method. Major and Minor range: 5000. Seed: 50

1.3.1 Object modeling method

The Object modeling method is used to model the channel facies. The Object modeling method is a more accurate facies modeling method compared to Sequential Indicator Simulation, because it allows creating actual subsurface objects, by using data from the well logs (Caers, 2005).

To create a channel model using Object modeling method a set of parameters describing the channel geometry is required: Channel width, channel wavelength, channel amplitude and channel thickness. Overall scheme of channel parameters is described in Figure 14.

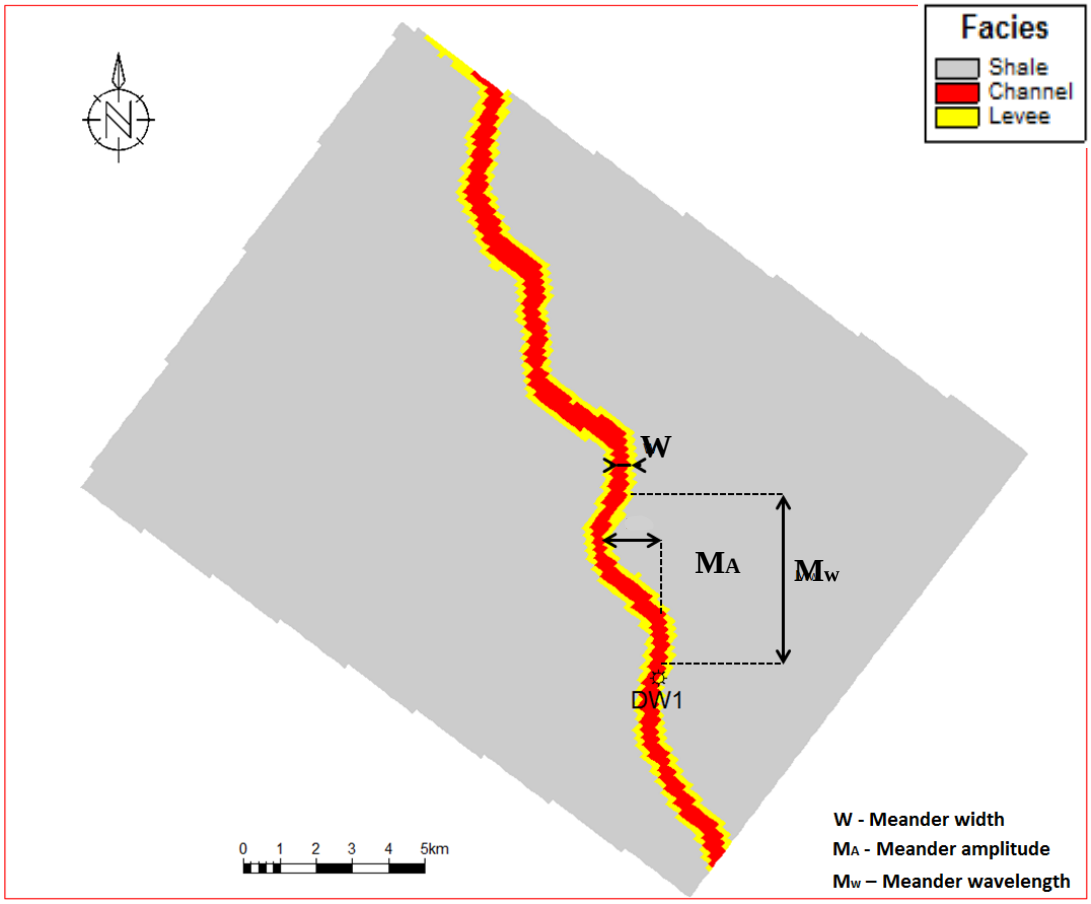

Figure 14: Map view description of channel parameters

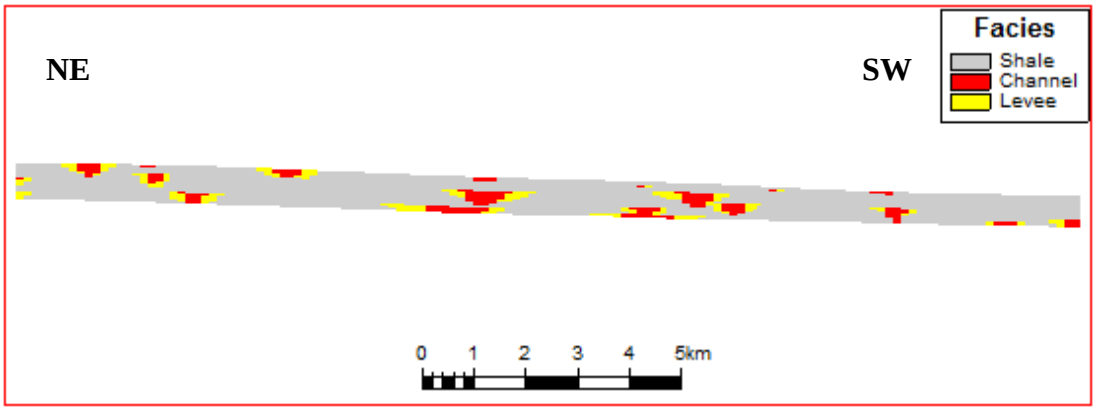

Figure 15: Cross-section of the channelized model

According to the Figure a range of modeling parameter values are taken into consideration, listed in (Table 1):

Channel parameters in meters	Min	Max
Thickness	10	70
Width	60	960
Amplitude	110	610
Wavelength	400	10400

Table 1: Range of modeling parameters according to the graph produced by (Leeder, 1973)

Each channel parameter has an influence on the model. Therefore, Figures 16 - 23 are showing these influences:

Channel thickness variations

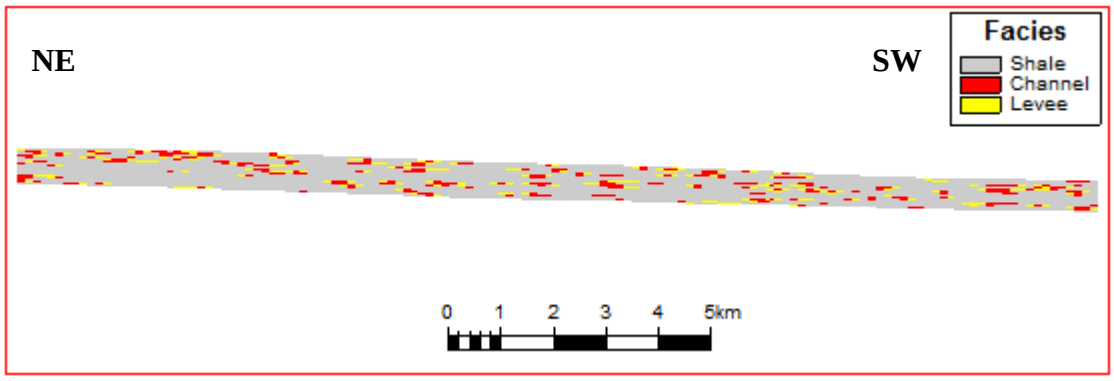

Figure 16: Cross section of the channelized model. Channel thickness 10m

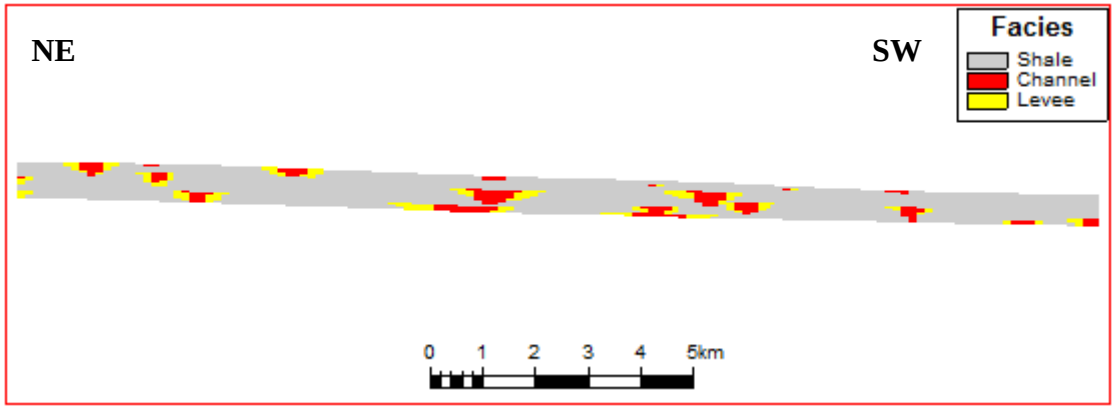

Figure 17: Cross section of the channelized model. Channel thickness 70m

Channel width variations

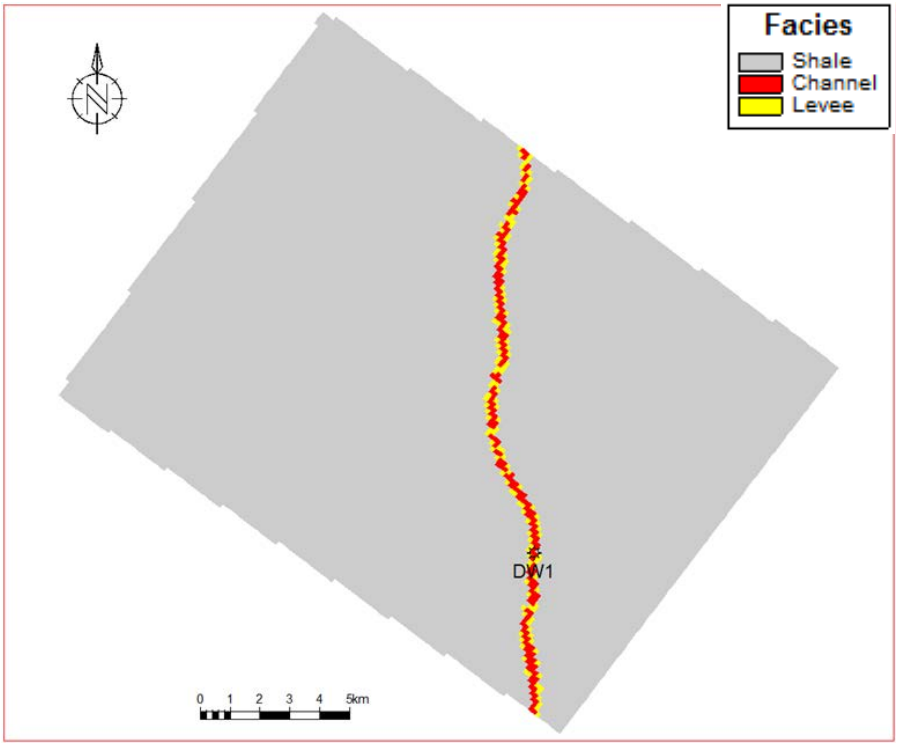

Figure 18: Channel width 60m

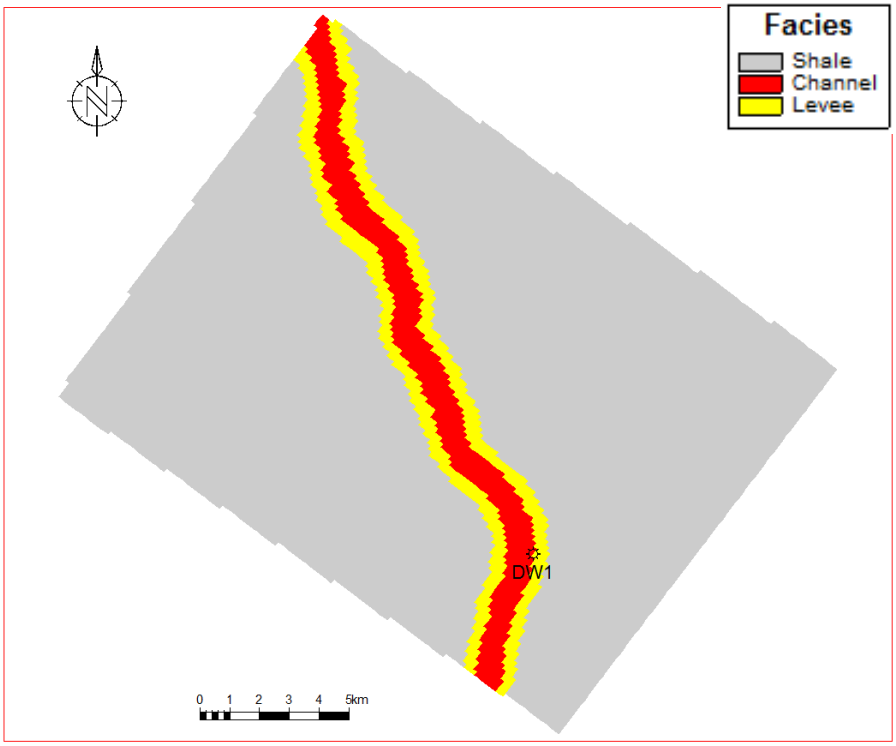

Figure 19: Channel width 960m

Channel amplitude variations

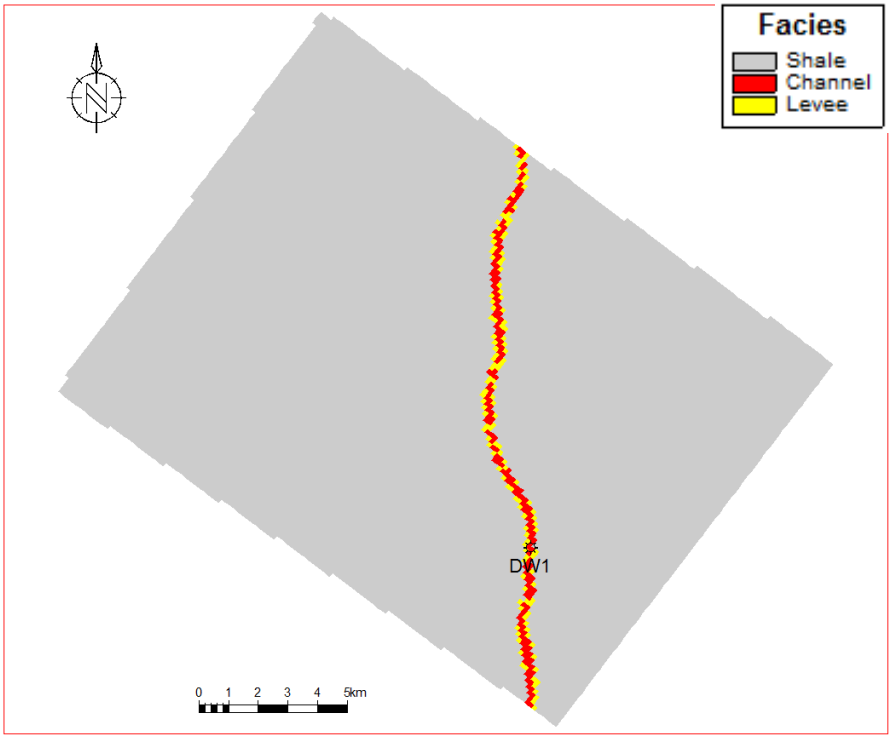

Figure 20: Channel amplitude 110m

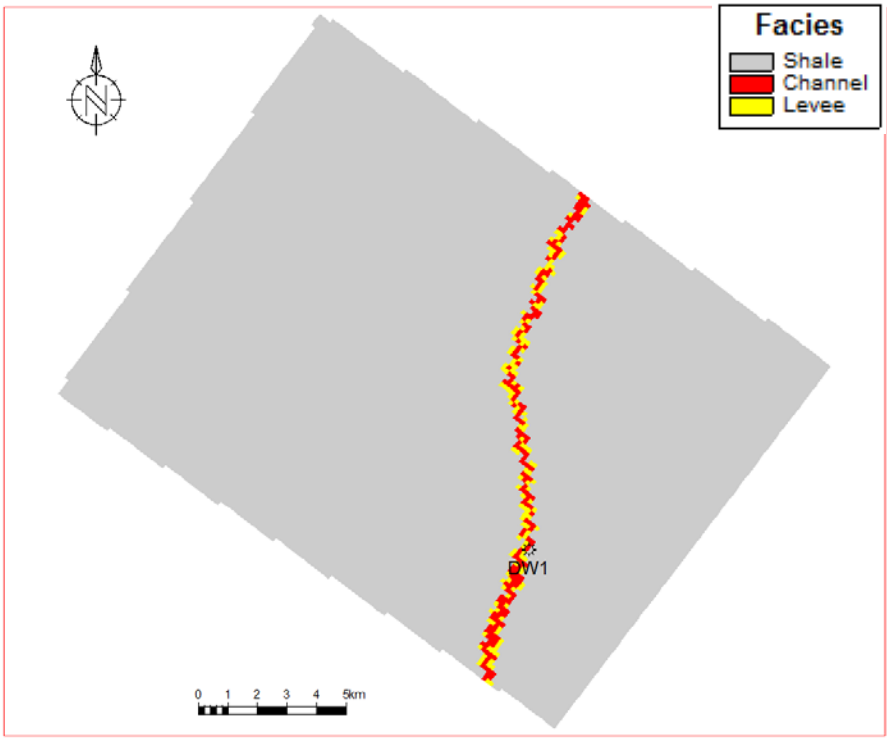

Figure 21: Channel amplitude 610m

Channel wavelength variations

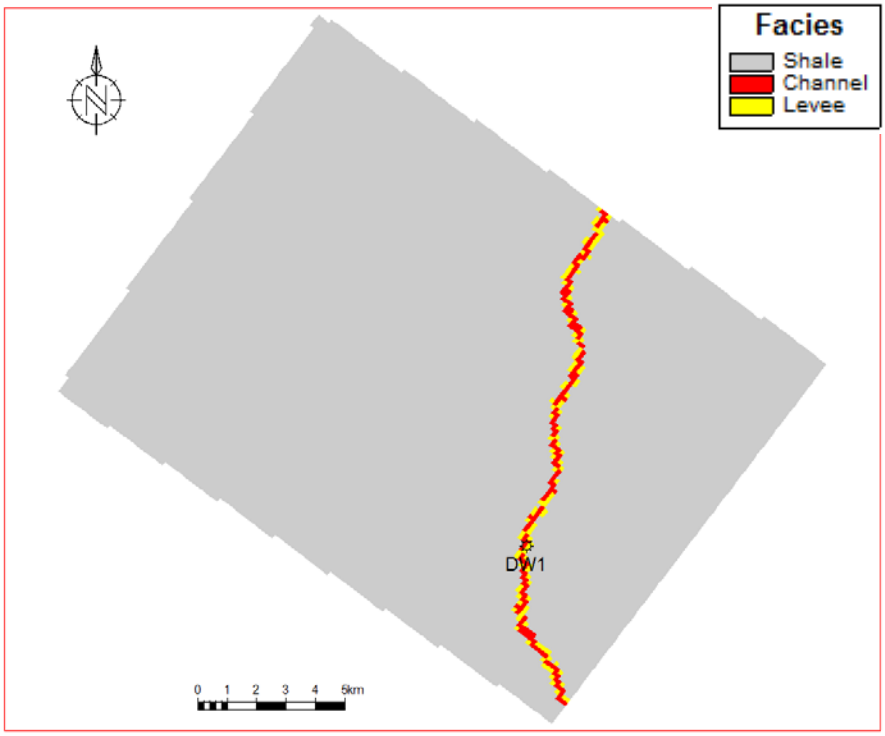

Figure 22: Channel wavelength 400m

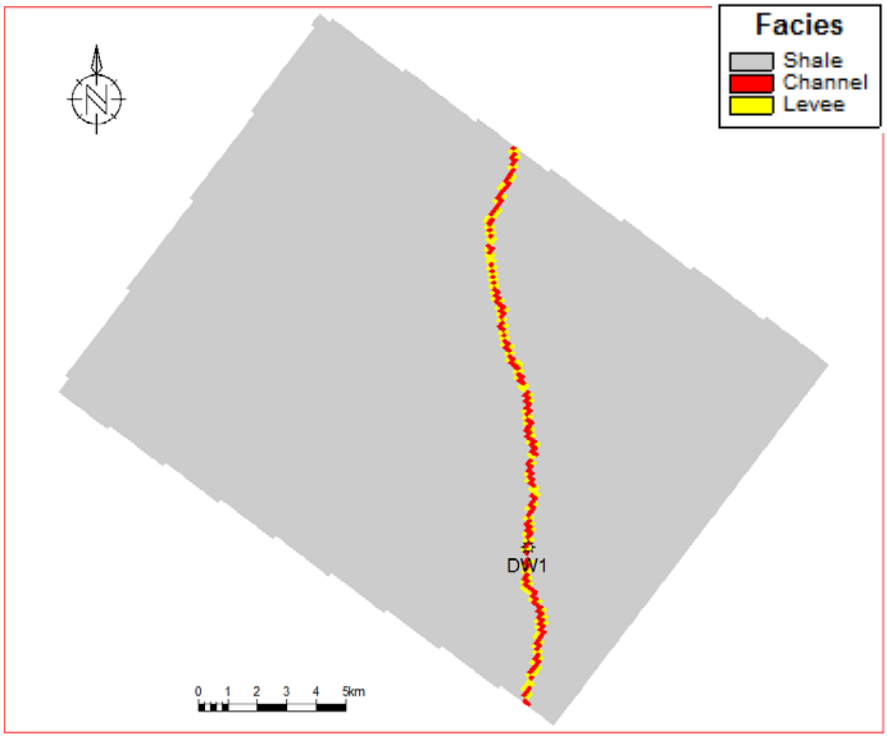

Figure 23: Channel wavelength 10400m

The Seed number controls the location of the channels. As it can be seen from the Figure 24 and Figure 25, the meander channel changes its direction of flow, when changing the Seed number.

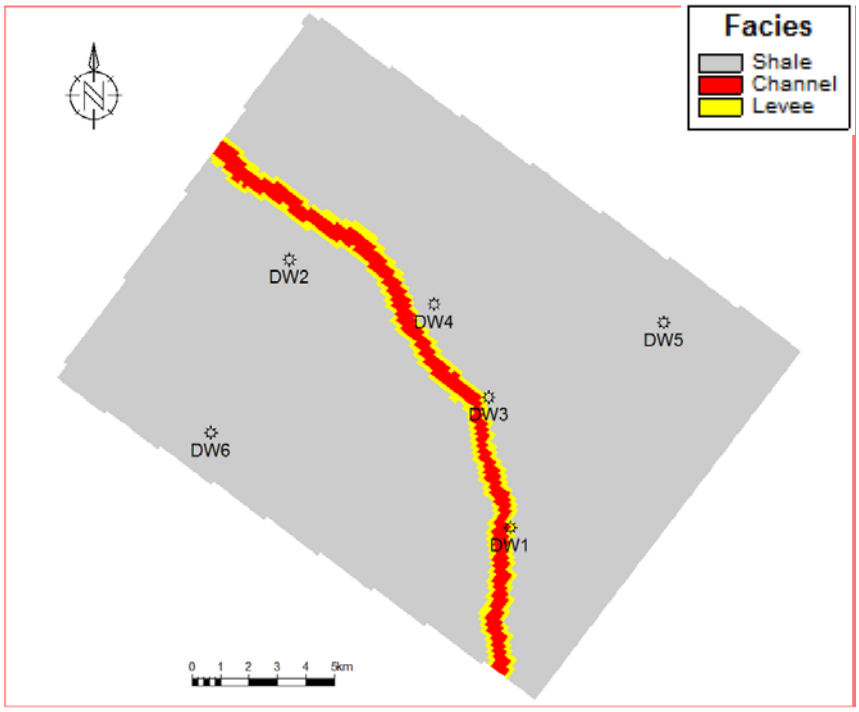

Figure 24: Object modeling method. Seed number 1

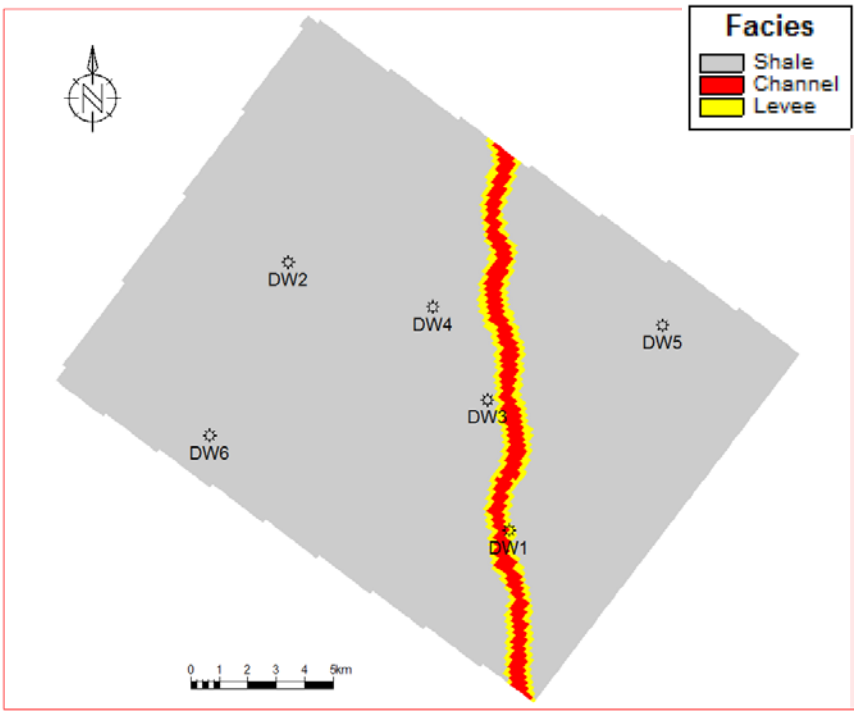

Figure 25: Object modeling method. Seed number 10

1.3.2 Influence of Sequential Indicator Simulation modeling parameters on reservoir volume distribution

The process of analyzing the influence of Sequential Indicator Simulation modeling requires some data preparation:

1. *Simplified facies*

In order to simplify the investigation, two facies are derived from the VSH (Volume of shale): reservoir and non-reservoir (Figure 26)

2. *Area of interests*

It is assumed, that reservoir models of different sizes have different influence on the reservoir volume uncertainty. To investigate this theory, several reservoir polygons were created. To keep the model as simple as possible, the shapes of these polygons are circular. To investigate the impact of the reservoir polygon size on the reservoir volume spread, it was decided to create a small (polygon with radius 500m) and a big (polygon with radius 1000m). In addition it is investigated, whether there is a significant influence of location of the polygon with respect to the well DW 1, on the reservoir volume spread.

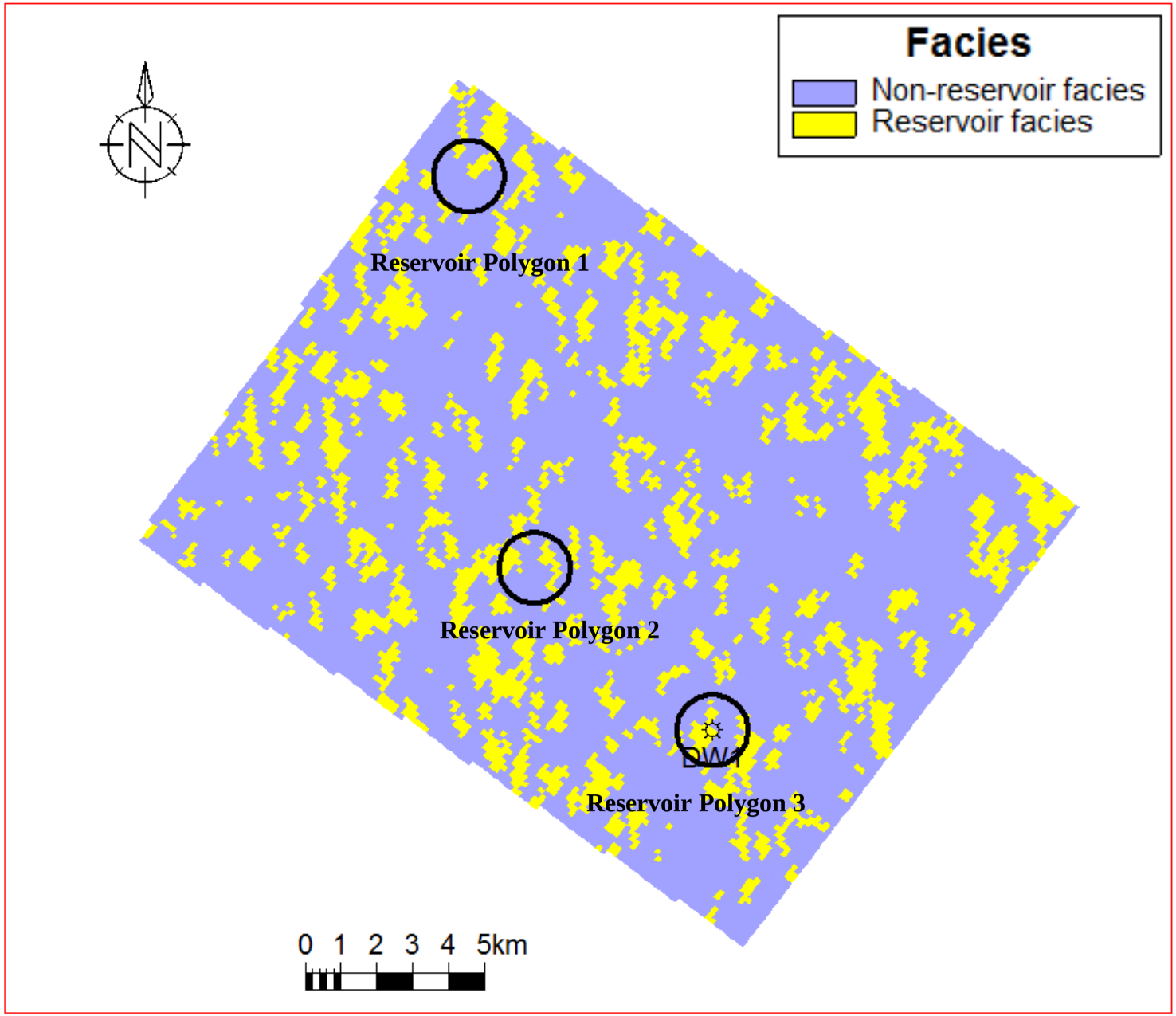

Figure 26: Conceptual model with reservoir and non-reservoir facies. Location of three circular reservoir polygons

The volume spread uncertainty calculation, is following the next workflow scheme outlined in the (Figure 27). This scheme consists of several steps:

- Define a variogram range – define horizontal and vertical anisotropy ranges
- Set a SEED number
- Calculate reservoir volume spread
- Repeat the last 2 steps 100 times, using different SEED numbers
- Change one parameter at a time – changing one parameter, keeping the other parameters constant

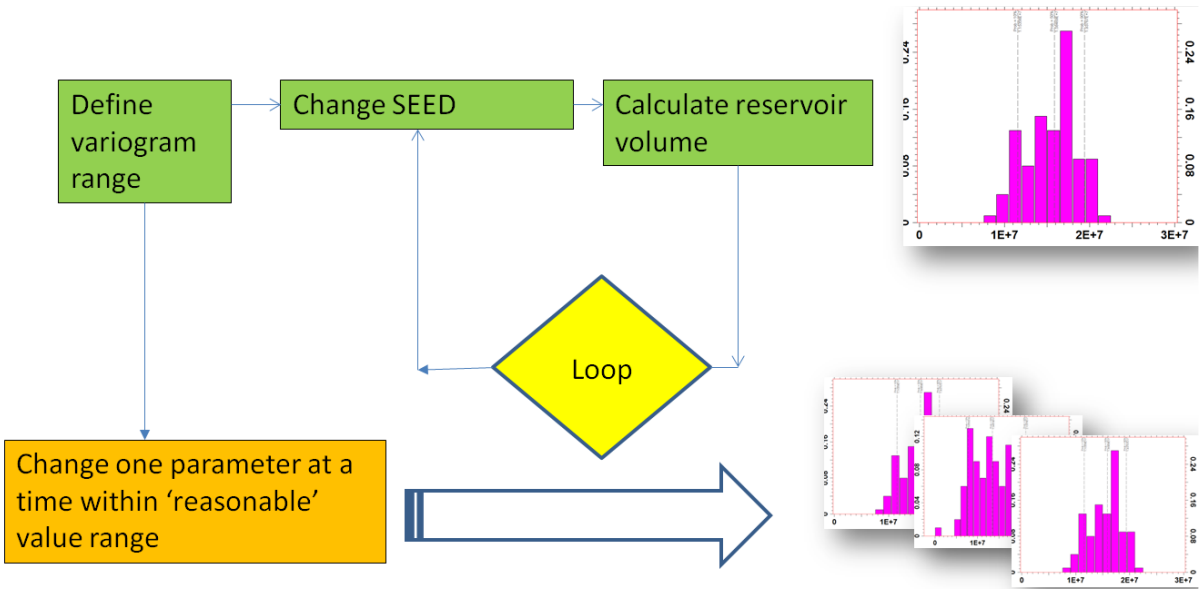

Figure 27: Sequential Indicator Simulation method workflow.

Note that the volume distribution for each set of parameters is calculated just thru changing the "*Seed*", which controls the location, of the reservoir and non-reservoir facies.

For calculation of the reservoir volume spread, the following formula is used:

$$\underline{Volume\ spread = (P90-P10)/P50*100}$$

P10, P50 and P90 values are taken from the reservoir volume spread CDF (Cumulative Distribution Function) shown in (Figure 28)

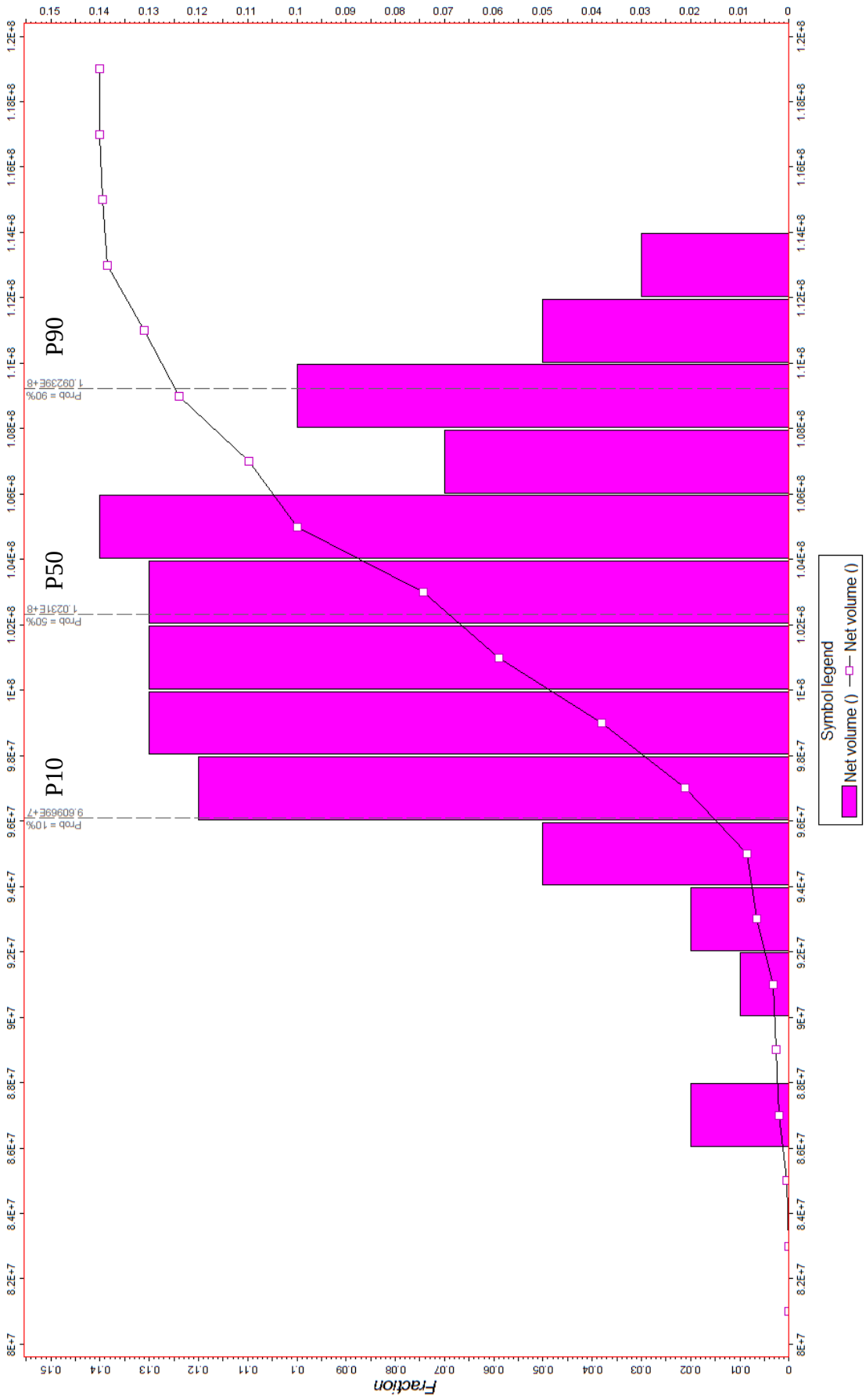

Figure 28: Reservoir volume distribution CDF (Cumulative Distribution Function) graph

1.3.3 Influence of Object modeling method parameters on reservoir volume spread

The Reservoir volume spread calculations based on Object modeling method will follow the next workflow (Figure 29):

- Define channel parameter – channel thickness, channel width, channel amplitude or channel wavelength
- Change SEED number
- Calculate reservoir volume spread
- Repeat last 2 steps 100 times, using different 100 SEED numbers
- Change one channel parameter at a time within reasonable value range

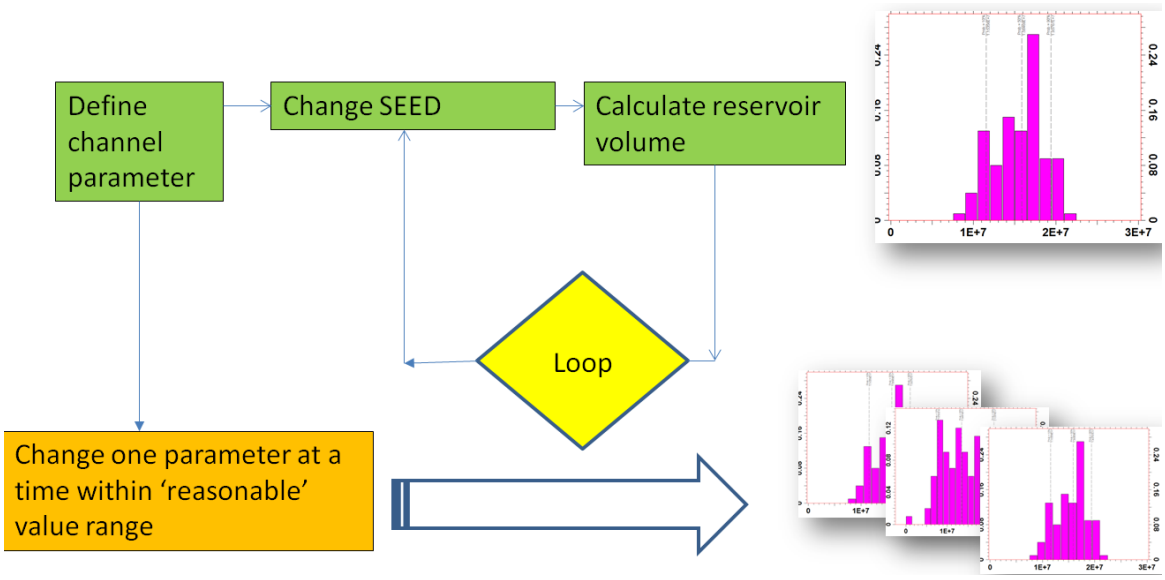

Figure 29: Object modeling method workflow

The goal of the work flow is to study the influence of the individual channel parameters on the reservoir volume distribution.

These parameters are: Channel width and depth, channel sinuosity, wavelength and amplitude. Following the steps outlined for Sequential Indicator Simulation the influence of these parameters on the reservoir volume uncertainty will be analyzed. According to the graph published by (Leeder, 1973), the value range of channel width for different channel depths is estimated and used for analysis (Figure 30).

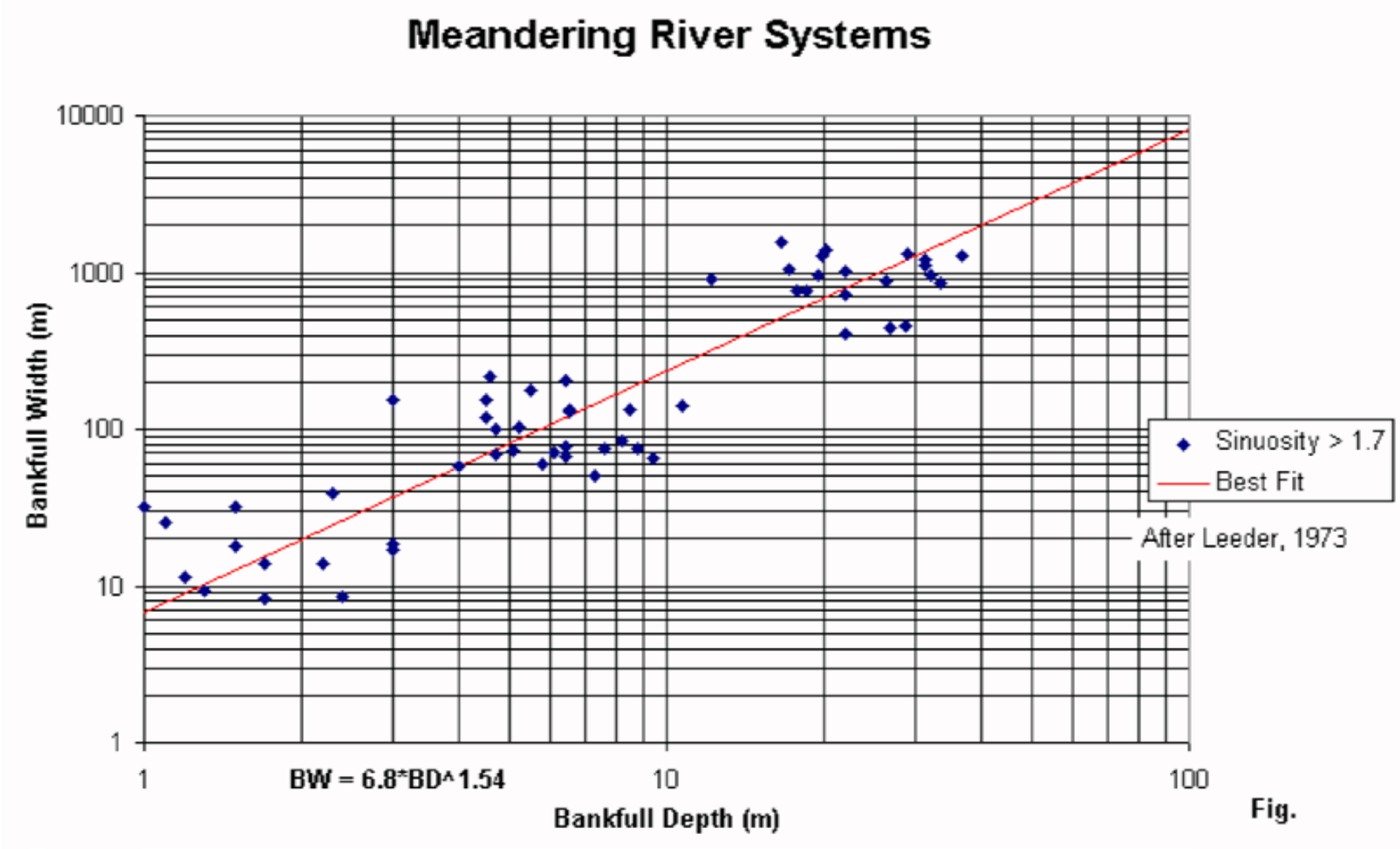

Figure 30: (Leeder, 1973) published data from modern high sinuosity rivers (>1.7) on the relationship between Channel Depth and Channel Width

The Figure 30 is showing the ratio of the meander channel width vs channel depth (thickness) ratio. The data-points presented in the graph are showing the relationship between the channel width and channel thickness, in different meandering channels in UK. For this particular project, the thickness of the channels varies from 10m – 70m and therefore, the range of the values for the width of the channel has a range from 60m – 960m. In Figure 31, data published by (Leopold and Wolman, 1960) and (Carlston, 1965) relates the width of the channel to the width of the meander-belt (channel-belt). According to the minimal channel width, channel amplitude is given the range from 110m – 610m. (Wonham et al., 2000) published a graph in which is shown the some actual statistical data of wavelength, with minimum channel width 60m. Therefore the range of the wavelength for this particular width varies from 400m – 10400m (Figure 32).

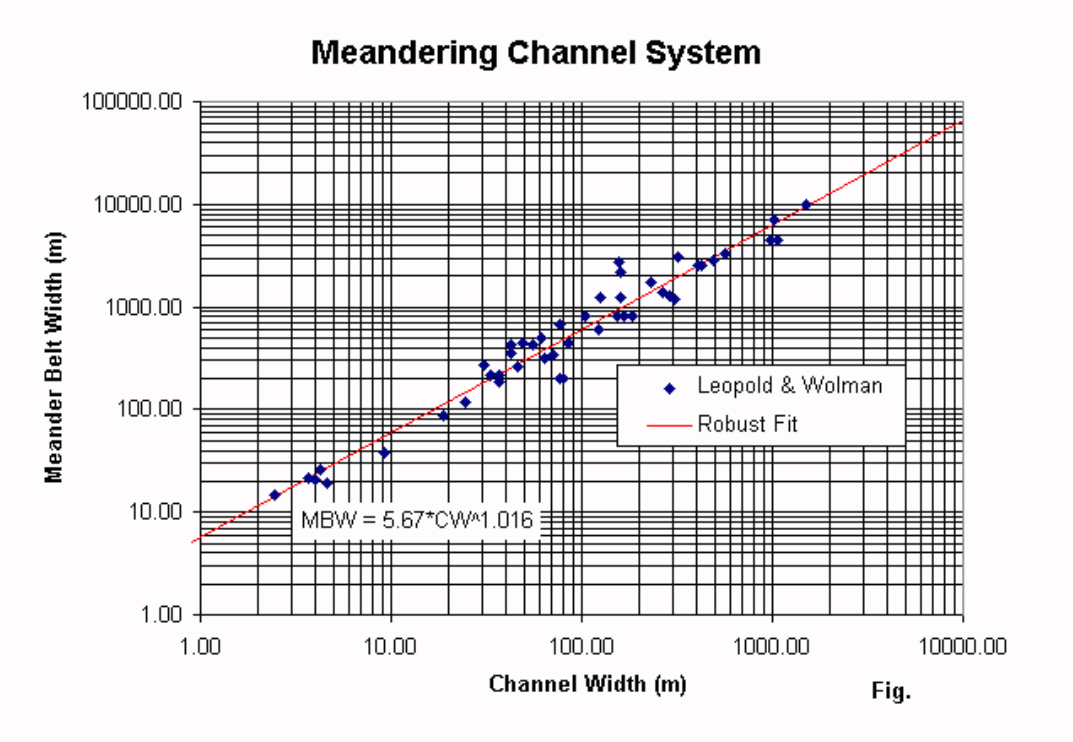

Figure 31: Data published by (Leopold and Wolman, 1960) and (Carlston, 1965). The ratio of meander belt width (Meander amplitude) vs channel width.

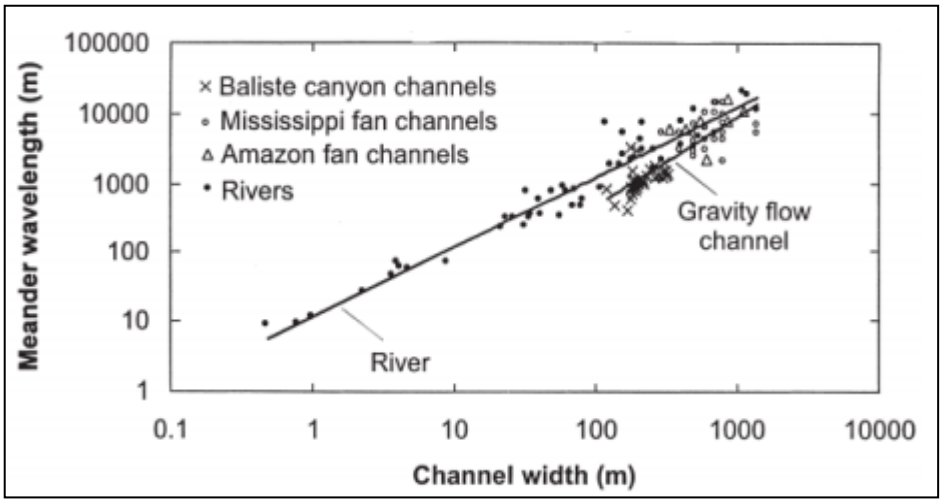

Figure 32: Data published by (Wonham et al., 2000). The ratio of channel width vs meander wavelength.

1.3.4 Acoustic impedance

The seismic acoustic impedance cube represents an approximation of the rock parameter acoustic impedance (Becquey et al., 1979) (Figure 33). It uses reservoir and non-reservoir facies probability data as a function of acoustic impedance responses (Figure 34). The facies impedance relationship is used as a look-up table for getting the sand-shale probability for a grid cell. This is done in the following way: each grid cell has an acoustic impedance value. The sand-shale probability is taken from the look-up table at this grid cell impedance value. Taken from Figure 33, the impedance range of 6500 (Pa*s/m) – 7500 (Pa*s/m) gives a sand probability of 56% and a shale probability of 44%. Instead of the global fraction derived from the wells these probabilities are used for building the cumulative distribution function for grid cells far away from the wells. The facies assigned to the grid cell is derived via a random number generator in a similar way as described in paragraph *Sequential Indicator Simulation* above.

The workflow for the Sequential Indicator Simulation based on the Seismic acoustic impedance cube is the same, as for Sequential Indicator Simulation modeling discussed above:

- Define a variogram range – define horizontal and vertical anisotropy ranges
- Change SEED number
- Calculate reservoir volume spread
- Repeat last 2 steps 100 times, using different 100 SEED numbers
- Change one parameter at a time – changing one parameter, while other parameters are remain still

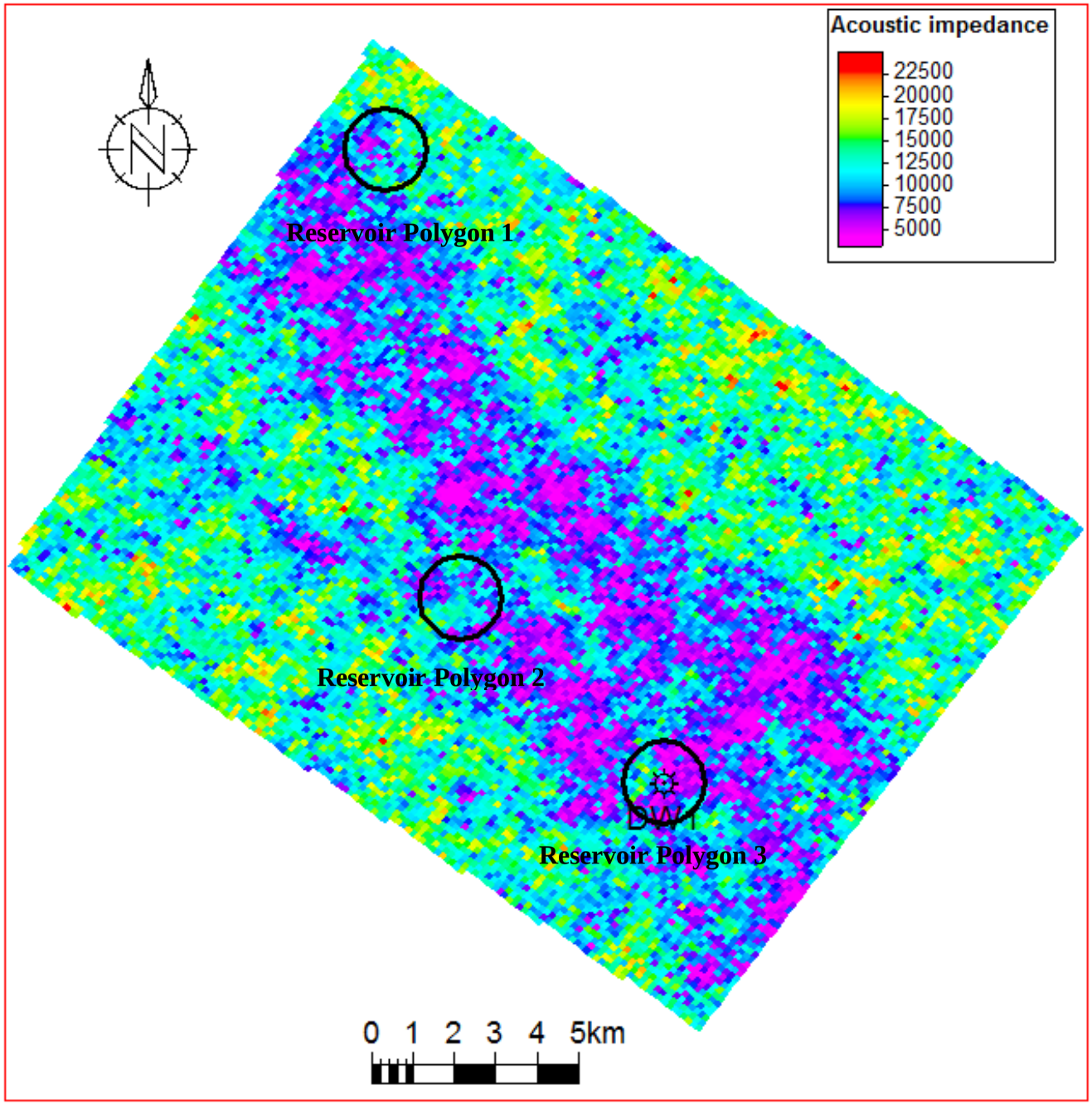

Figure 33: The Seismic acoustic impedance cube

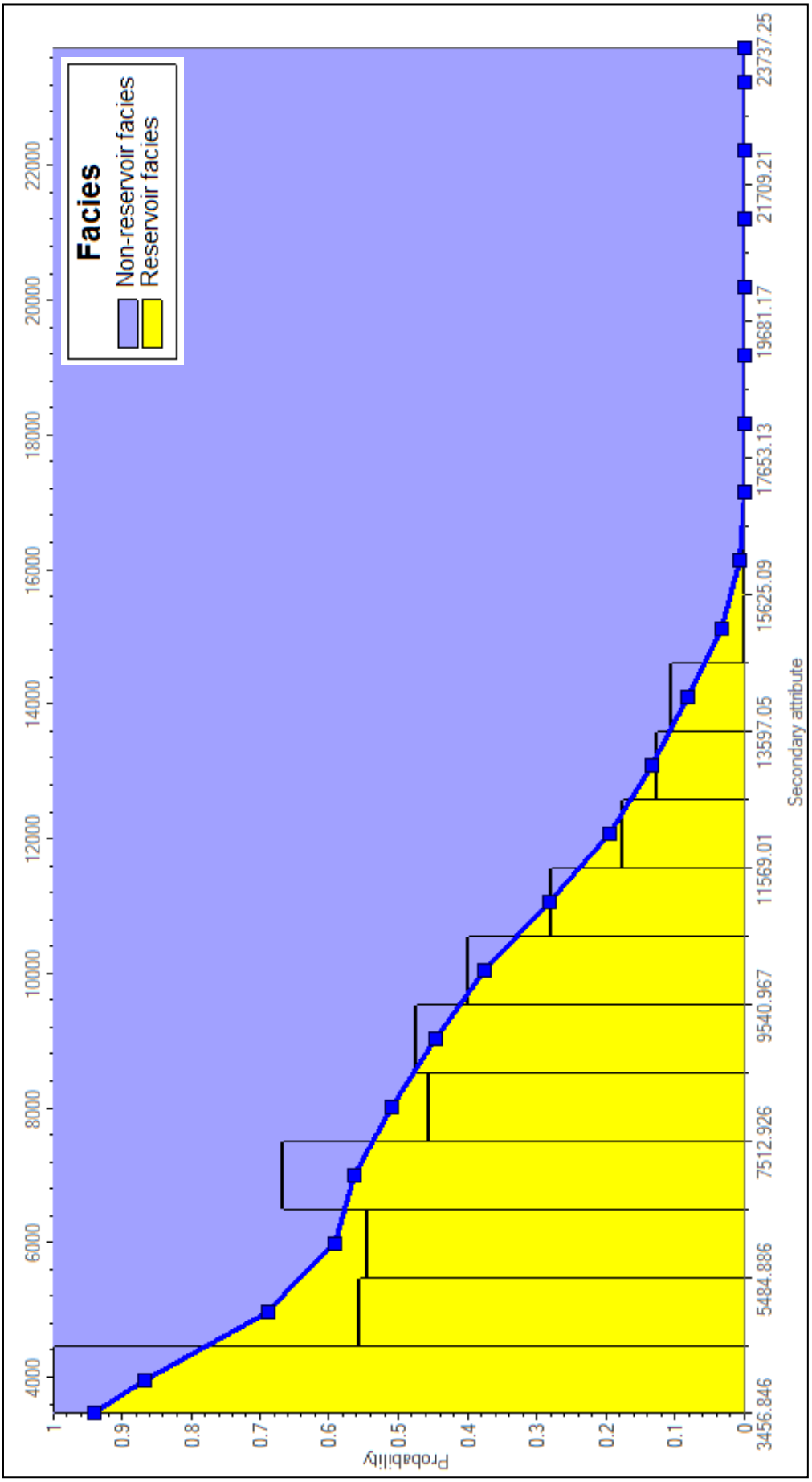

Figure 34: Reservoir facies probability distribution, according to acoustic impedance responses

Chapter 2 : OBSERVATIONS

2.1 Sequential Indicator Simulation

First the reservoir volume spread observations are done for reservoir polygon 3, which is located around the well (Figure 35)

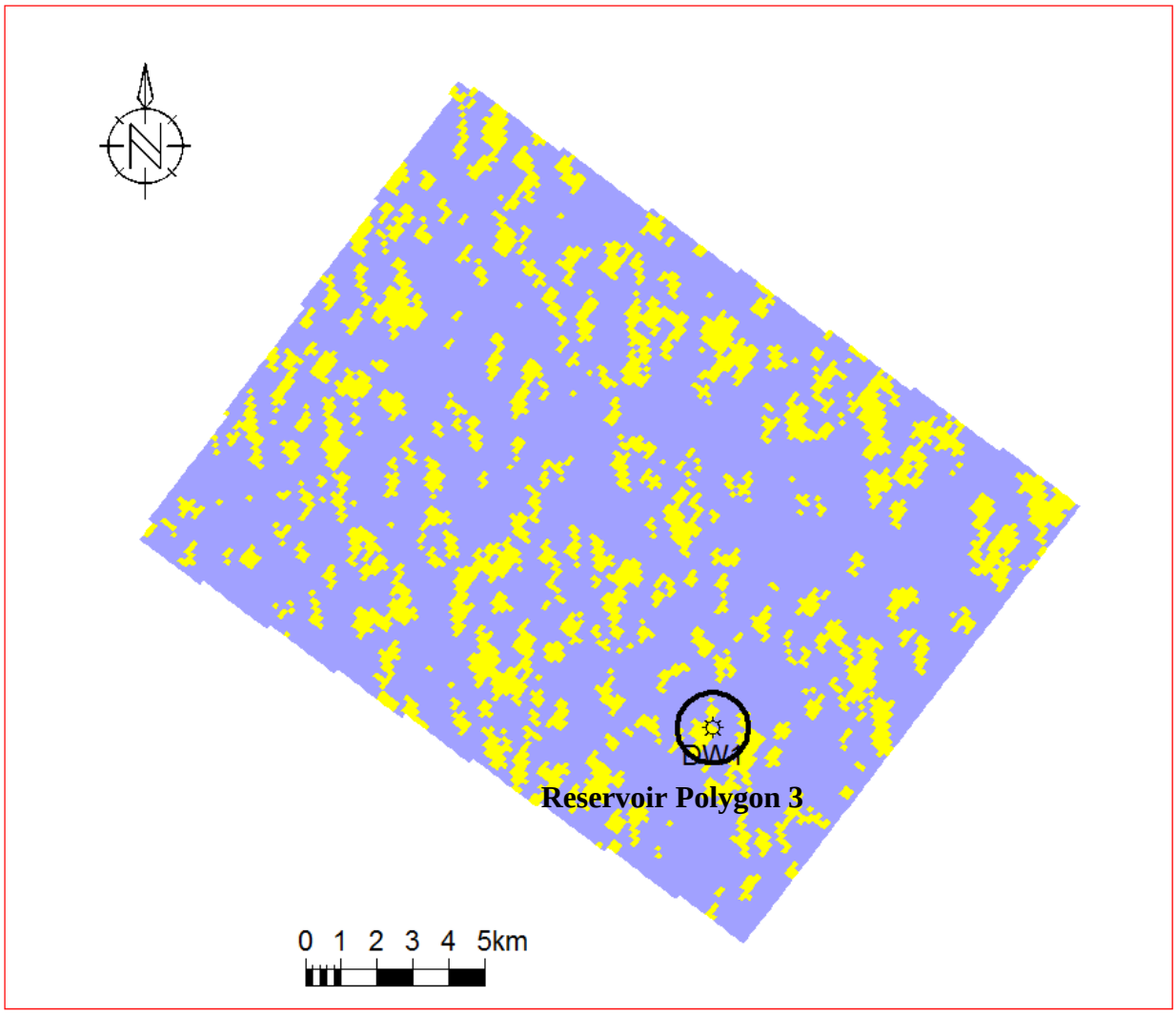

Figure 35: Location of reservoir polygon 3

As shown in Figure 36a and Figure 36b, the volume spread distributions for two polygons with radius 500m and 1000m, were plotted as a function of the horizontal variogram ranges, where the major range and minor range, have the same value. Color coded are the reservoir volume spread functions for the three vertical ranges: 1m, 10m and 50m. The reservoir volume spread calculations in Figure 36a and Figure 36b are made for polygon 3, which is located around the well.

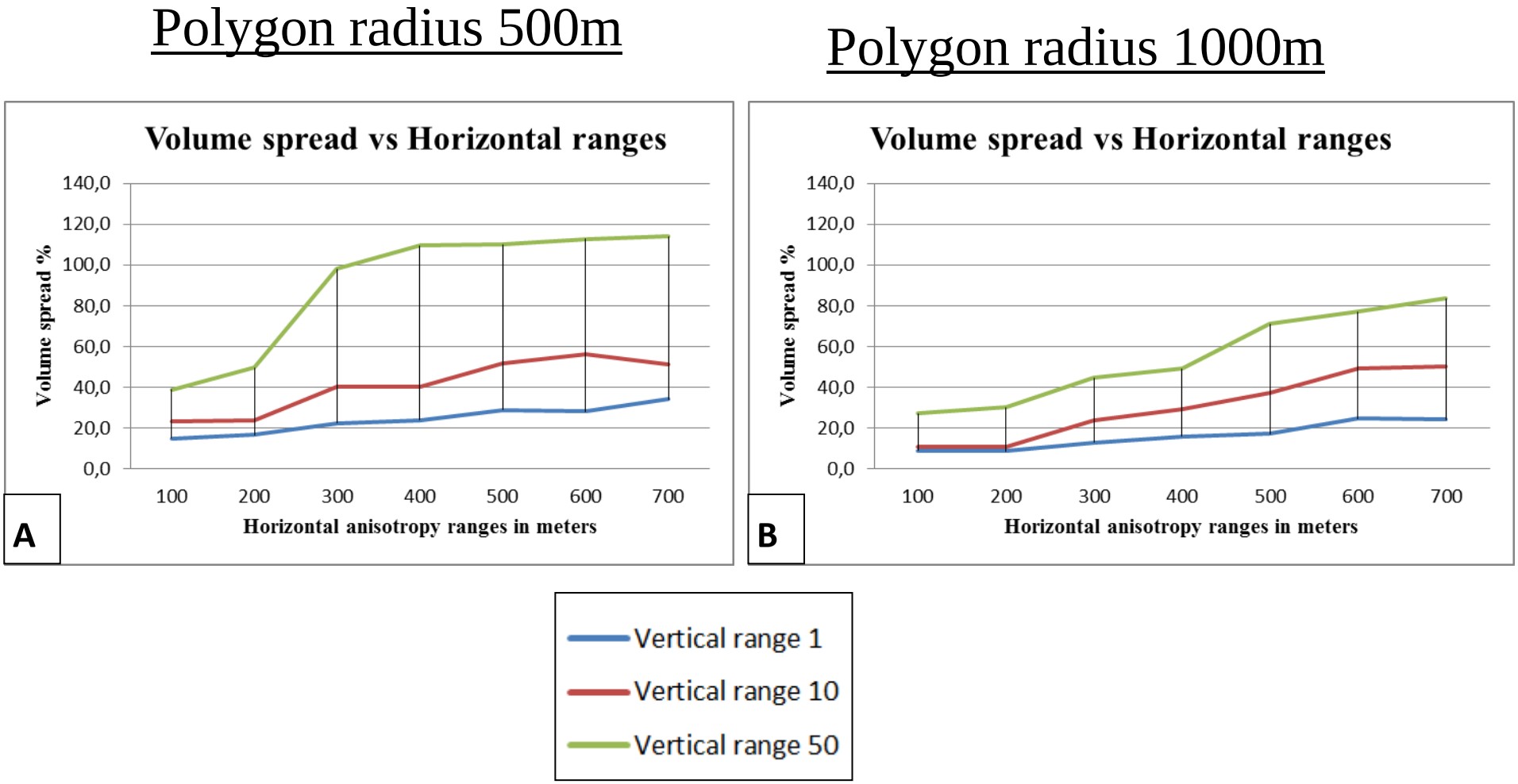

Figure 36: a) Reservoir volume spread distributions for polygon with radius 500m using different vertical ranges. b) Reservoir volume spread distributions for polygon with radius 1000m using different vertical ranges.

The volume spread for the vertical variogram range of 50m and the polygon with radius 500m shows the largest volume spread with increasing horizontal variogram range. For a small horizontal range (100-200m) the reservoir volume spread is around 40%, then the volume spread increases till 100% for the horizontal range of 300m. The volume spread increases slowly, reaching 114% for a horizontal range of 700m. For the vertical range of 1m and 10m, the reservoir volume spread is much lower. For the vertical range of 10m it increases from 23% for the horizontal range of 100m, till 51% for the horizontal range of 700m. The vertical range of 1m shows a volume spread function with the smallest values, giving 15% for the horizontal range of 100m, and increases till 34% at horizontal range of 700m. The results for the reservoir polygon with radius 500m are given in Table 2:

SIS Polygon radius 500m		
Varioqram ranges	100m	700m
Vertical range 1	40 %	114 %
Vertical range 10	23 %	51 %
Vertical range 50	15 %	34 %

Table 2: Sequential Indicator Simulation: volume spreads for polygon 3, with radius 500m.

As stated previously, the reservoir volume spread for the reservoir polygon with radius 1000m shows a lower volume spread compared to the polygon with radius 500m., The reservoir volume spread for the vertical range 50m increases from 27% for the horizontal range of 100m to 84% for the horizontal range of 700m. The volume spread for the vertical ranges 10m and 1m are around 10% for the horizontal range of 100m. The volume spread increases up to 50% and 24%, for the horizontal range of 700m, and a vertical range of 10m and 1m respectively. The results for the reservoir polygon with radius 1000m are given in Table 3:

SIS Polygon radius 1000m		
Varioqram ranges	100m	700m
Vertical range 1	27 %	84 %
Vertical range 10	10 %	50 %
Vertical range 50	10 %	24 %

Table 3: Sequential Indicator Simulation: volume spread for polygon 3, with radius 1000m

The reservoir volume spread seems to be sensitive to the variogram ranges, when the size of the reservoir is small. This is nicely observed in Figure 36a, where the increasing horizontal and vertical ranges, affect considerably the reservoir volume spread. In Figure 36b, the influence of the reservoir

size on the reservoir volume spread is much smaller, compared to the reservoir polygon with radius 500m.

In Figure 37a, the reservoir volume spread functions for the three polygons with radius 500m are plotted, as a function of the horizontal variogram range, where the major and minor range have the same values. The vertical range is set to 10m. Figure 37b shows the three polygons together with the position of the well and also showing a Sequential Indicator Simulation result of the reservoir (sand) facies. Polygon 1 is located far away from the wells, polygon 2 is located close to the wells and polygon 3 is located around the well. Figure 37a shall show the influence of the position of a well with respect to the reservoir location on the volume spread. It was decided to make the calculations on the reservoir polygons with radius 500m because the reservoir volume spread function is more sensitive to variogram ranges for a small reservoir size. The three functions of the Figure 37a show the volume spread for the three polygons.

For the horizontal range of 100m, the reservoir volume spread for all three polygons is about 24%. . The trend of the reservoir volume spread is increasing, delivering 81%, 69% and 51%, for the horizontal range of 700m and the three reservoir polygons (Table 4). Note that the volume spread for polygon1 (far away from the well) shows the largest volume spread values, whereas the polygon 3 (positioned around the well) is giving the smallest numbers for the different horizontal variogram range. The volume spread functions for the polygons with a vertical range of 1m and 50m confirms this result.

SIS Polygon radius 500m		
Varioqram ranges	100m	700m
Polygon 1	24 %	81 %
Polygon 2	24 %	69 %
Polygon 3	24 %	51 %

Table 4: Sequential Indicator Simulation: volume spread function for the polygons 1, 2 and 3, with radius 500m.

Polygon radius 500m

Position of reservoirs

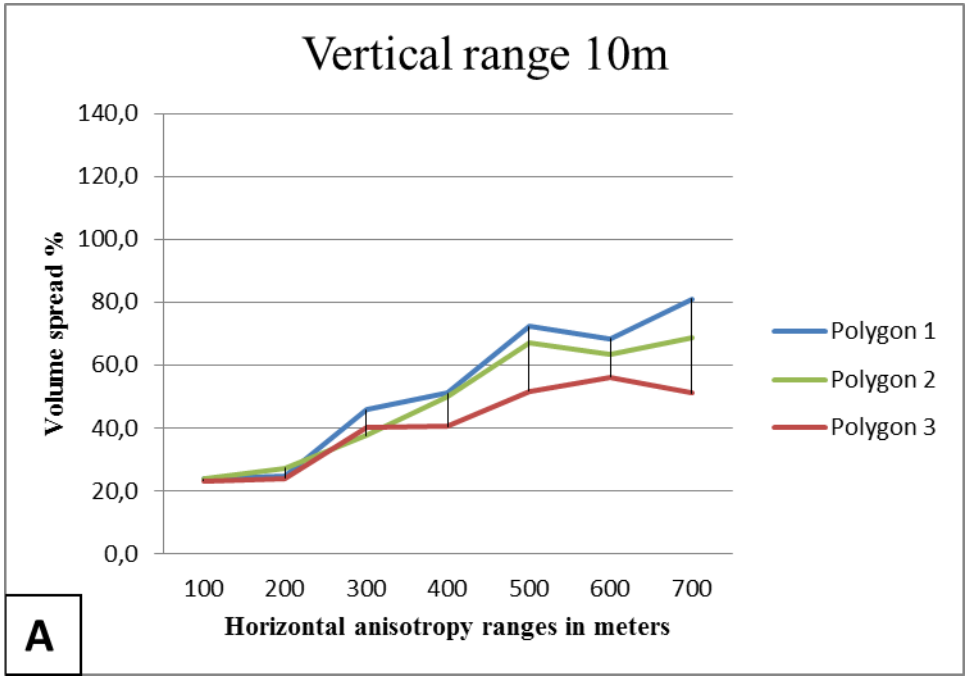

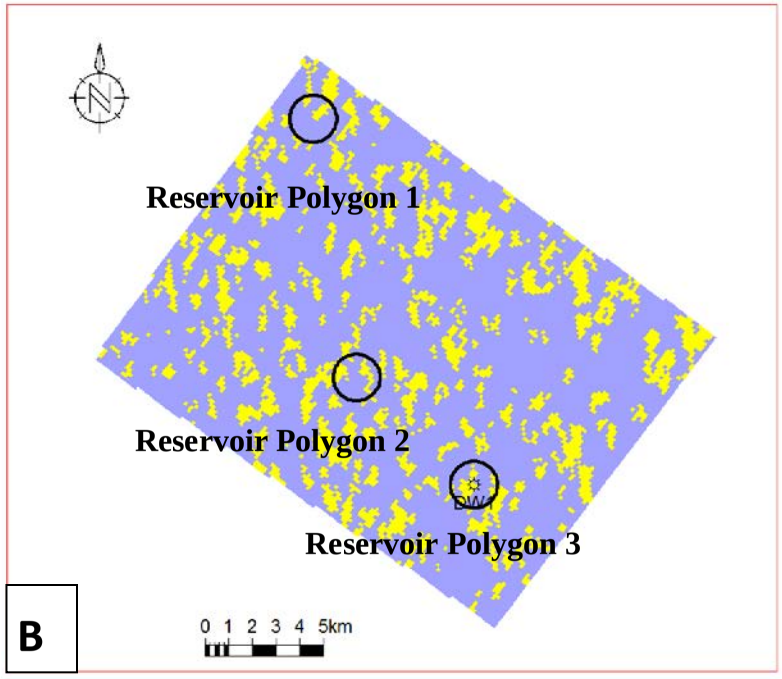

Figure 37: a) Reservoir volume spread distributions for different polygons with radius 500m. b) Sequential Indicator Simulation model of reservoir facies, with the position of the reservoir polygons.

The results of further investigation of the reservoir size influence on the reservoir volume spread function are summarized in Figure 38. This figure shows the reservoir volume spread as a function of the horizontal variogram range, where again the major and minor range have the same values. The vertical variogram range is set to 50m. The reservoir volume spread functions are shown for the polygon 3 located around the well and with a radius of 500m and 1000m.

The volume spread functions for both polygons are increasing with increasing horizontal range. , The volume spread for the polygon with radius 1000m increases gradually from 27% at horizontal range 100m, to 84% at horizontal ranges 700m. The reservoir volume spread function for the polygon with radius 500m shows higher values, starting around 40% for a horizontal range of 100m, and increasing to 114% for the horizontal ranges of 700m (Table 5).

Varioqram ranges	100m	700m
Polygon radius 500m	40 %	114 %
Polygon radius 1000m	27 %	84 %

Table 5: Sequential Indicator Simulation volume spread for polygon 3, with radius 500m and 1000m.

Obviously the size of the reservoir polygon influences the reservoir volume spread function. The Figure 38 supports the theory of getting a high reservoir volume spread for a small reservoir and a large variogram range.

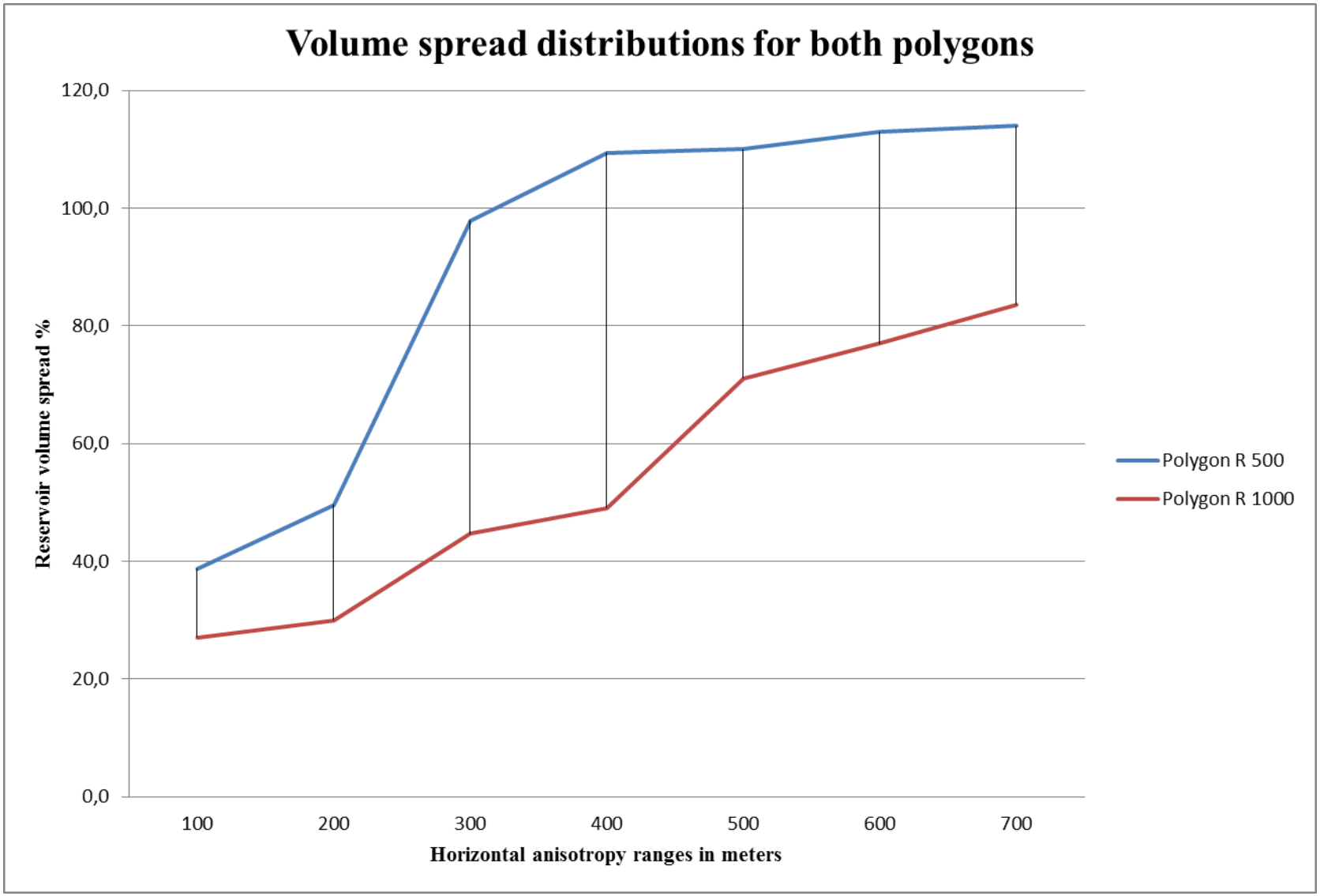

Figure 38: Reservoir volume distribution graphs for polygon 3 with radius 500m and 1000m.

To observe the sensitivity of the reservoir volume spread on horizontal variogram ranges of different values (anisotropy), the Figure 39a and Figure 39b were plotted. In both figures the volume spread distributions were plotted for the reservoir polygon 3 around the well with radius 500m, as a function of the horizontal anisotropy ranges. In figure 39a the major and minor ranges have the same value, and in figure 39b they deviate by 30% Color coded are the reservoir volume spread functions for the three vertical ranges: 1m, 10m and 50m. In both Figures the reservoir volume spread function for a vertical range of 50m, shows the largest values. The volume spread function for the vertical range of 1m shows the smallest values. Figure 39a shows an increase in volume spread for vertical range of 50m, from 40% at horizontal ranges 100m, to 114% at horizontal range of 700m (Table 6). In Figure 39b the volume spread increases from 47%, to 106%, at horizontal ranges 100m and 700m respectively (Table 7).

Major range = Minor range		
Varioqram ranges	100m	700m
Vertical range 1m	15 %	34 %
Vertical range 10m	23 %	54 %
Vertical range 50m	40 %	114 %

Table 6: Sequential Indicator Simulation volume spread for polygon 3, using "Major range = Minor range", and vertical ranges: 1m, 10m and 50m.

MInor range = 70%Major range		
Varioqram ranges	100m	700m
Vetical range 1m	15 %	34 %
Vertical range 10m	24 %	44 %
Vertical range 50m	47 %	106 %

Table 7: Sequential Indicator Simulation volume spread for polygon 3, using "Minor range = 70%Major range", and vertical ranges: 1m, 10m and 50m.

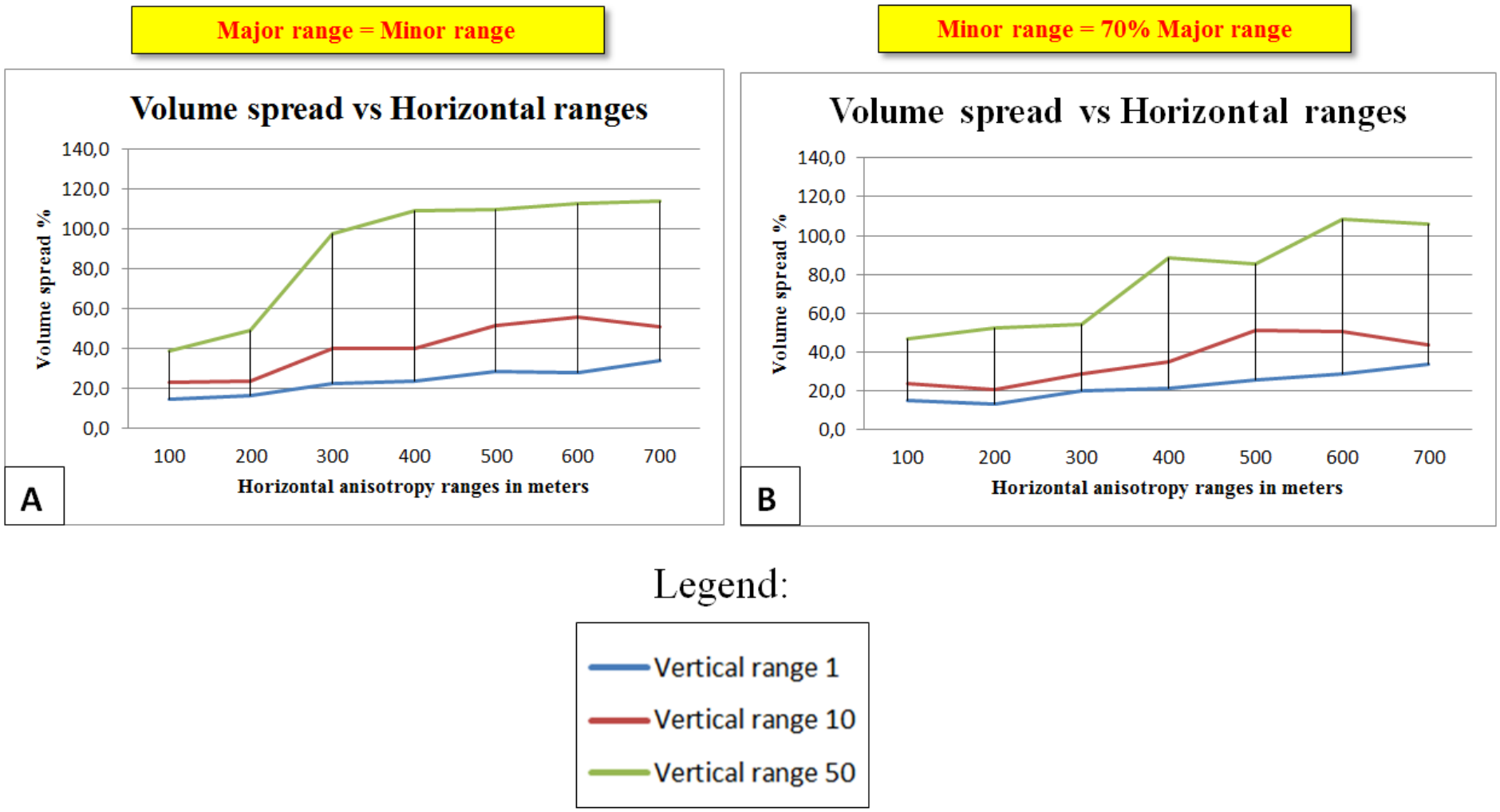

Figure 39: a) Reservoir volume spread distributions for polygon 3 with radius 500m using equal horizontal ranges. b) Reservoir volume spread distributions for polygon 3 with radius 1000m using different horizontal ranges.

To investigate and compare the influence of horizontal anisotropy ranges on the reservoir volume spread function, several plots for polygon 3 have been made. Figure 40a and Figure 40b show the reservoir volume spread, as a function of horizontal anisotropy ranges. Color coded are the reservoir volume spread functions for equal horizontal ranges (blue) and for the case where the minor range constitutes 70% of the major range (red). The reservoir volume spread functions for the polygon with radius 500m are slightly higher compared to the reservoir volume spread for the reservoir polygon with radius 1000m. The results for the reservoir volume spread shown is Figure 40a and Figure 40b are given in Table 8 and Table 9:

SIS Polygon radius 500m		
Varioqram ranges	100m	700m
Major range = Minor range	39 %	114 %
Minor range = 70%Major range	47 %	106 %

Table 8: Sequential Indicator Simulation: volume spreads for polygon 3 with radius 500m using different horizontal ranges.

SIS Polygon radius 1000m		
Varioqram ranges	100m	700m
Major range = Minor range	27 %	87 %
Minor range = 70%Major range	20 %	80 %

Table 9: Sequential Indicator Simulation: volume spread for polygon 3 with radius 1000m, using different horizontal ranges

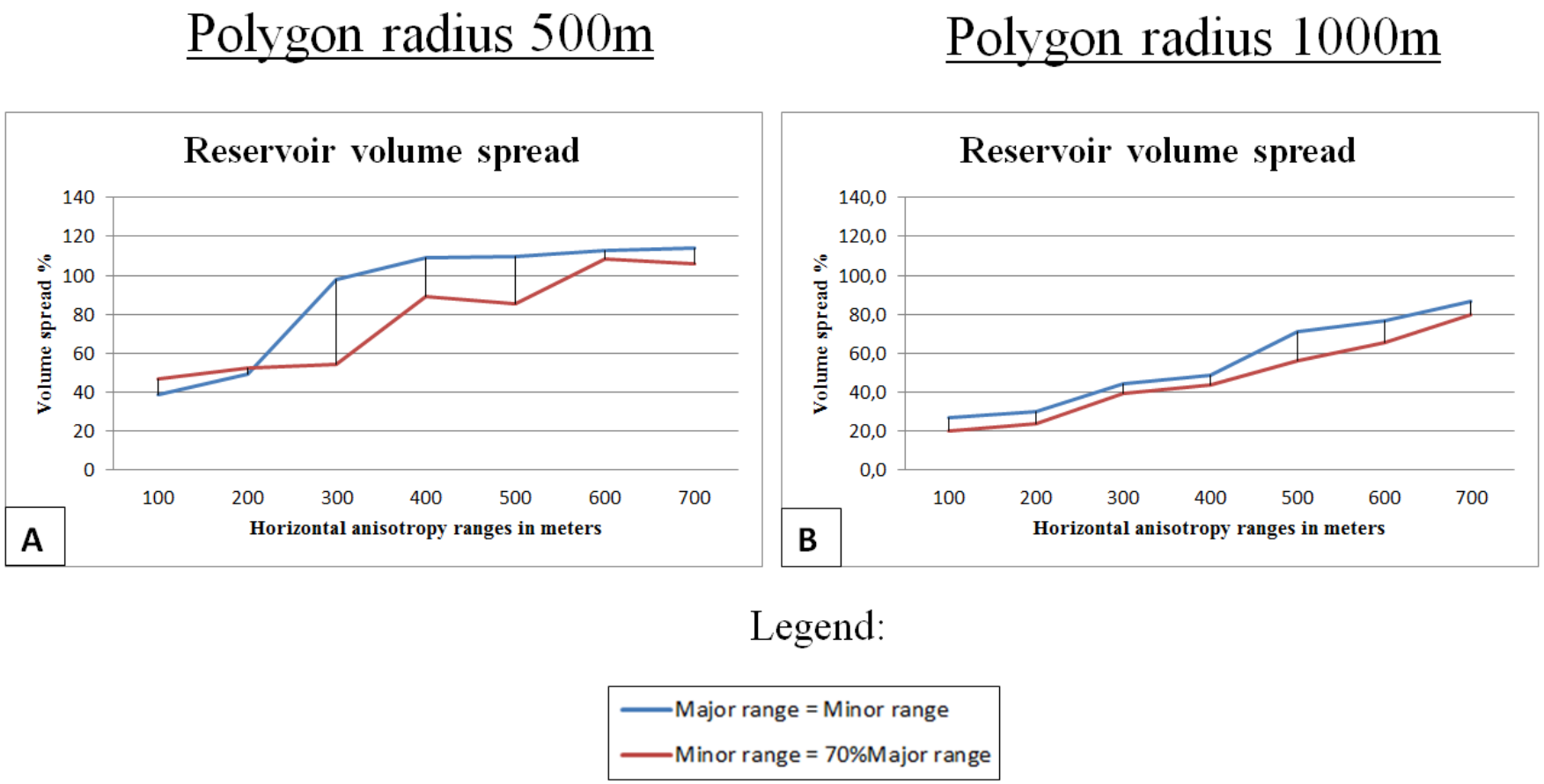

Figure 40: a) Reservoir volume spread distributions for polygon 3 with radius 500m using equal and different horizontal anisotropy ranges. b) Reservoir volume spread distributions for polygon 3 with radius 1000m using equal and different horizontal anisotropy ranges.

2.2 Object modeling method

To investigate the behavior of the reservoir volume spread for Object Modeling, the following channel parameters were investigated: Channel thickness, channel width, channel amplitude and channel wavelength. Following the publication of (Leeder 1973), the range of channel parameters used for reservoir volume spread analysis, was estimated from analogues.

In Figure 41a and Figure 41b the reservoir volume spread was derived for various channel thicknesses. The channel thickness was increased from 10m to 70m, while the other geometrical parameters were set to the values shown in Table 10.

Channel Thickness	10m - 70m
Channel Width	60m
Channel Amplitude	110m
Channel Wavelength	400m

Table 10: Channel thickness variations

Figure 41 shows an increasing trend of the reservoir volume spread with channel thickness for all 3 polygons. Among all three reservoir polygons, polygon 3, which is located around the well, shows a smaller increase with the channel thickness compared to the volume spread linked to the other polygons. The volume spread for the reservoir polygon of radius 500m shows a larger increase with increasing channel thickness compared to the reservoir polygon of 1000m radius. A summary of the volume spread is given in Table 11.

		Polygon 500m		Polygon 1000m	
	Channel Thickness	10m	70m	10m	70m
Volume spread %	Polygon 1	38	105,4	38	71,7
	Polygon 2	45,6	123,8	45,6	75,5
	Polygon 3	33,6	64,9	*33,6*	42,8

Table 11: Volume spread distribution for three polygons obtained by channel thickness variations

Figure 42 shows the reservoir volume spread for different channel width values ranging from 60m to 960m. All other parameters were set to the values shown in Table 12.

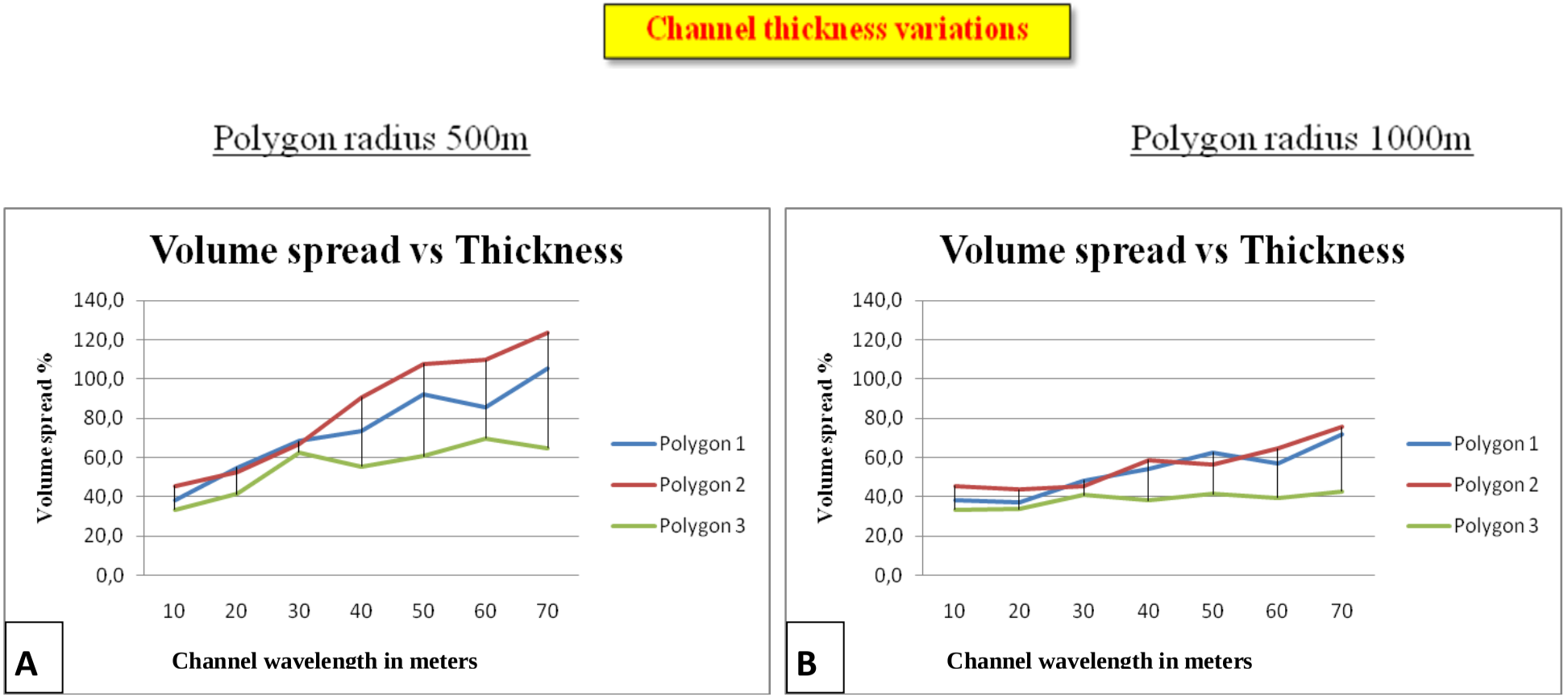

Figure 41: a) Volume spread distributions for three polygons with radius 500m, obtained by increasing the channel thickness. b) Volume spread distributions for three polygons with radius 1000m, obtained by increasing the channel thickness

Channel Thickness	10m
Channel Width	60m – 960m
Channel Amplitude	110m
Channel Wavelength	400m

Table 12: Channel width variations

In comparison to the previous graphs, in the Figure 42, the polygon 3 which is located around the well does not show a significant trend of reservoir volume spread. The reservoir volume spread for the other two polygons with radius with 500m shows larger increase, comparison to the reservoir volume spread in polygon with radius 1000m. A summary of the volume spread is given in Table 13.

		Polygon 500m		Polygon 1000m	
	Channel width	10m	70m	10m	70m
Volume spread %	Polygon 1	38,2	95,7	25,3	56,3
	Polygon 2	45,6	114,8	31,5	64,7
	Polygon 3	33,6	45,9	23	36,9

Table 13: Volume spread distribution for three polygons obtained by channel width variations

Figure 43 shows the reservoir volume spread function of the channel amplitude for the 3 polygons. The channel amplitude increases from 110m to 610m (Table 14). As the graphs for all six polygons show, there is no significant influence of the channel amplitude on reservoir volume spread.

Channel Thickness	10m
Channel Width	60m
Channel Amplitude	110m - 610m
Channel Wavelength	400m

Table 14: Channel amplitude variations

The reservoir polygons with radius 500m, show a volume spread between 30%-50% for the analyzed channel amplitudes, while the reservoir polygon with radius 1000m, deliver a reservoir volume spread around 30%.

Channel width variations

Polygon radius 500m

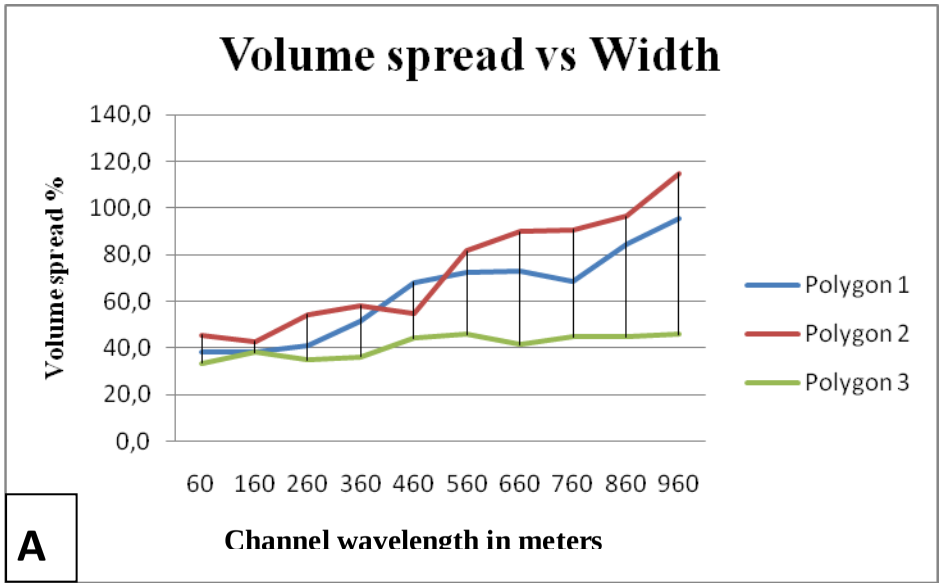

Polygon radius 1000m

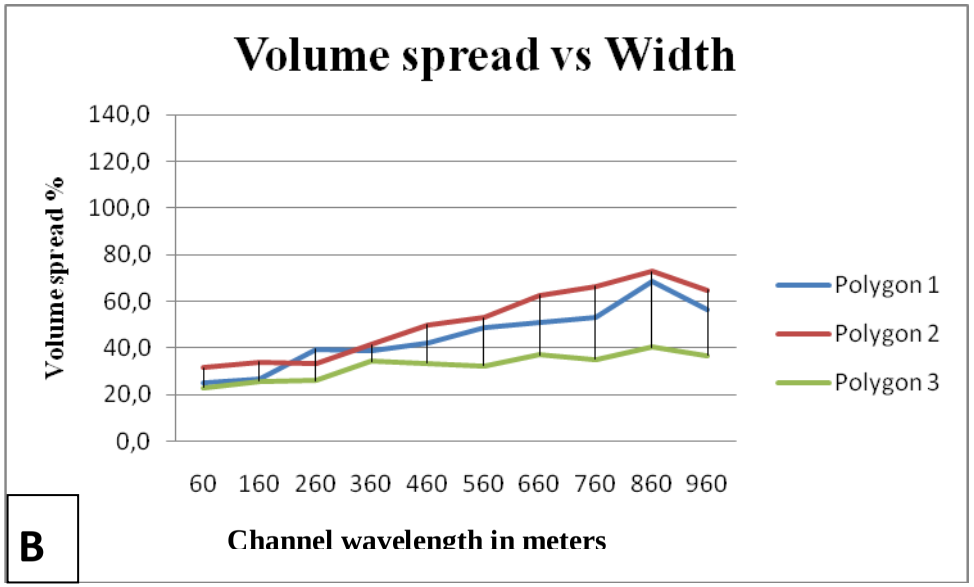

Figure 42: a) Volume spread distributions for three polygons with radius 500m, obtained by increasing the channel width. b) Volume spread distributions for three polygons with radius 1000m, obtained by increasing the channel width.

Channel amplitude variations

Polygon radius 500m

Polygon radius 1000m

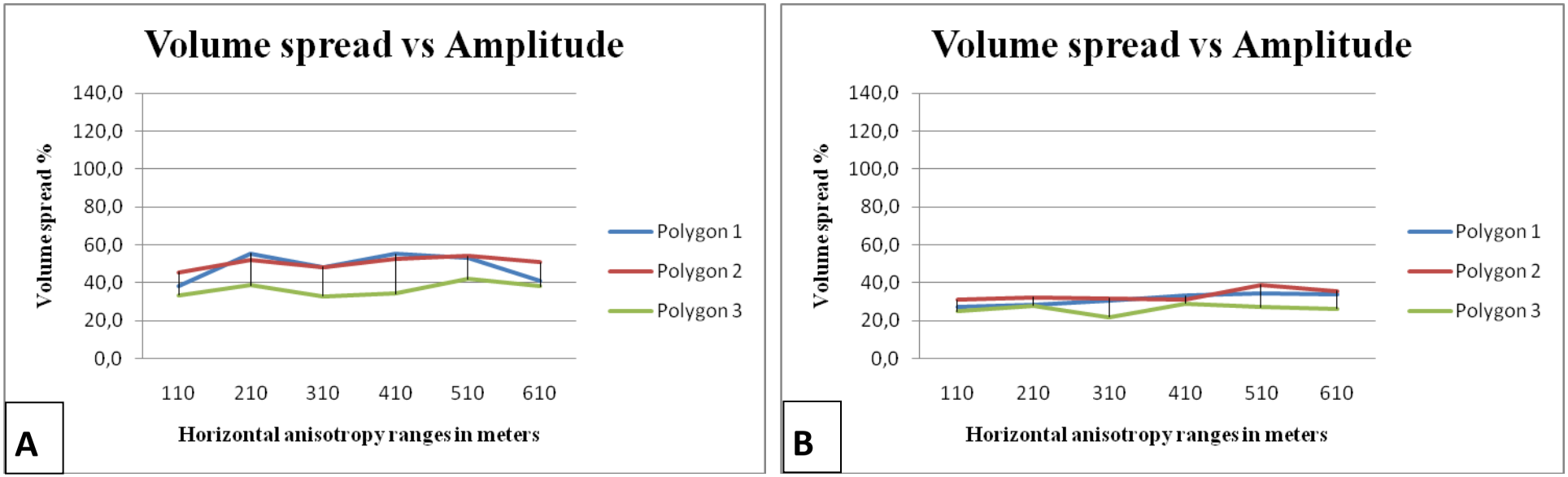

Figure 43: a) Volume spread distributions for three polygons with radius 500m, obtained by increasing the channel amplitude. b) Volume spread distributions for three polygons with radius 1000m, obtained by increasing the channel amplitude.

		Polygon 500m		Polygon 1000m	
	Channel amplitude	110m	610m	110m	610m
Volume spread %	Polygon 1	38,2	41,2	27,4	34
	Polygon 2	45,6	51	31	36
	Polygon 3	33,6	38,2	25	26,2

Table 15: Volume spread distribution for three polygons obtained by channel amplitude variations

The reservoir volume spreads of Figure 44, are obtained through increasing the channel wavelength from 400m to 10400m (Table 16). They show almost the same trend for all polygons, similar to figure 3 discussed in the previous graphs. For the polygons with radius 500m, the reservoir volume spread varies around 40%, whereas for the reservoir polygons with radius 1000m, the reservoir volume spread lies around 30% (Table 17).

Channel Thickness	10m
Channel Width	60m
Channel Amplitude	110m
Channel Wavelength	400m – 10400m

Table 16: Channel wavelength variations

		Polygon 500m		Polygon 1000m	
	Channel wavelength	400m	10400m	400m	10400m
Volume spread %	Polygon 1	33,2	40,2	25,4	24,3
	Polygon 2	45,6	51,9	32	30
	Polygon 3	33,6	39,9	24,5	25,6

Table 17: Volume spread distribution for three polygons obtained by channel wavelength

Channel wavelength variations

Polygon radius 500m

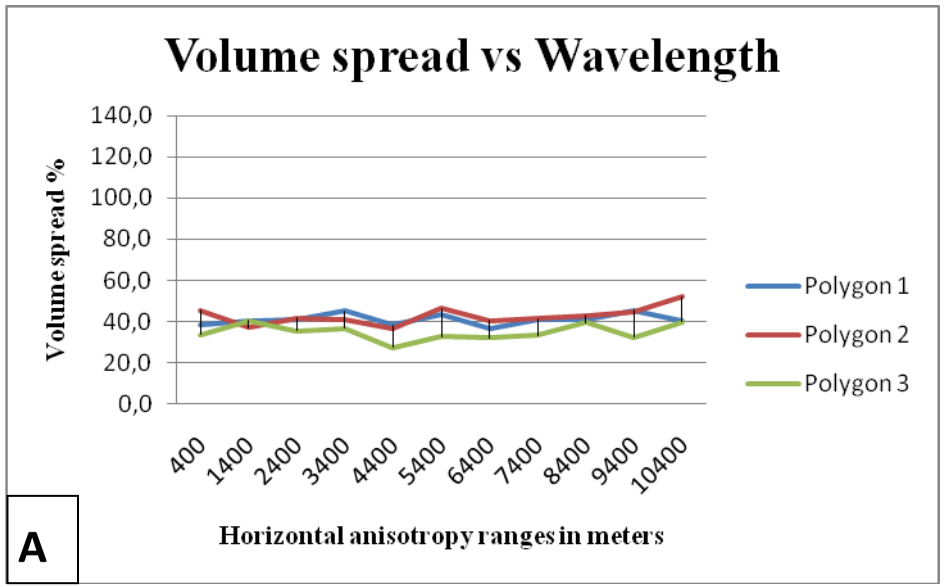

Polygon radius 1000m

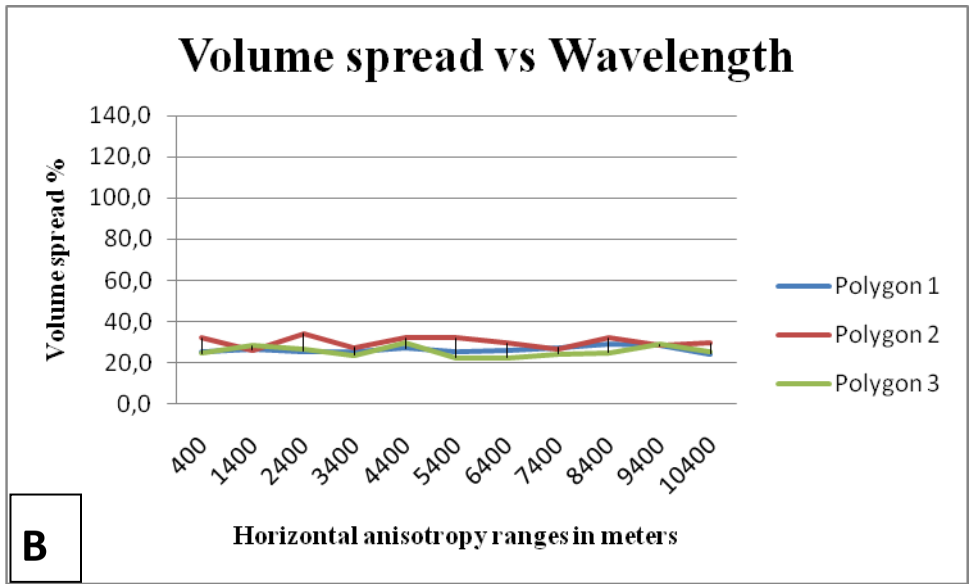

Figure 44: a) Volume spread distributions for three polygons with radius 500m, obtained by increasing the channel wavelength. b) Volume spread distributions for three polygons with radius 1000m, obtained by increasing the channel wavelength.

2.3 Acoustic impedance

As stated in previous chapter, a seismic acoustic impedance cube represents an approximation of the rock parameter acoustic impedance (Figure 45). This chapter mainly focuses on the influence of the seismic acoustic impedance cube on the reservoir volume spread distribution.

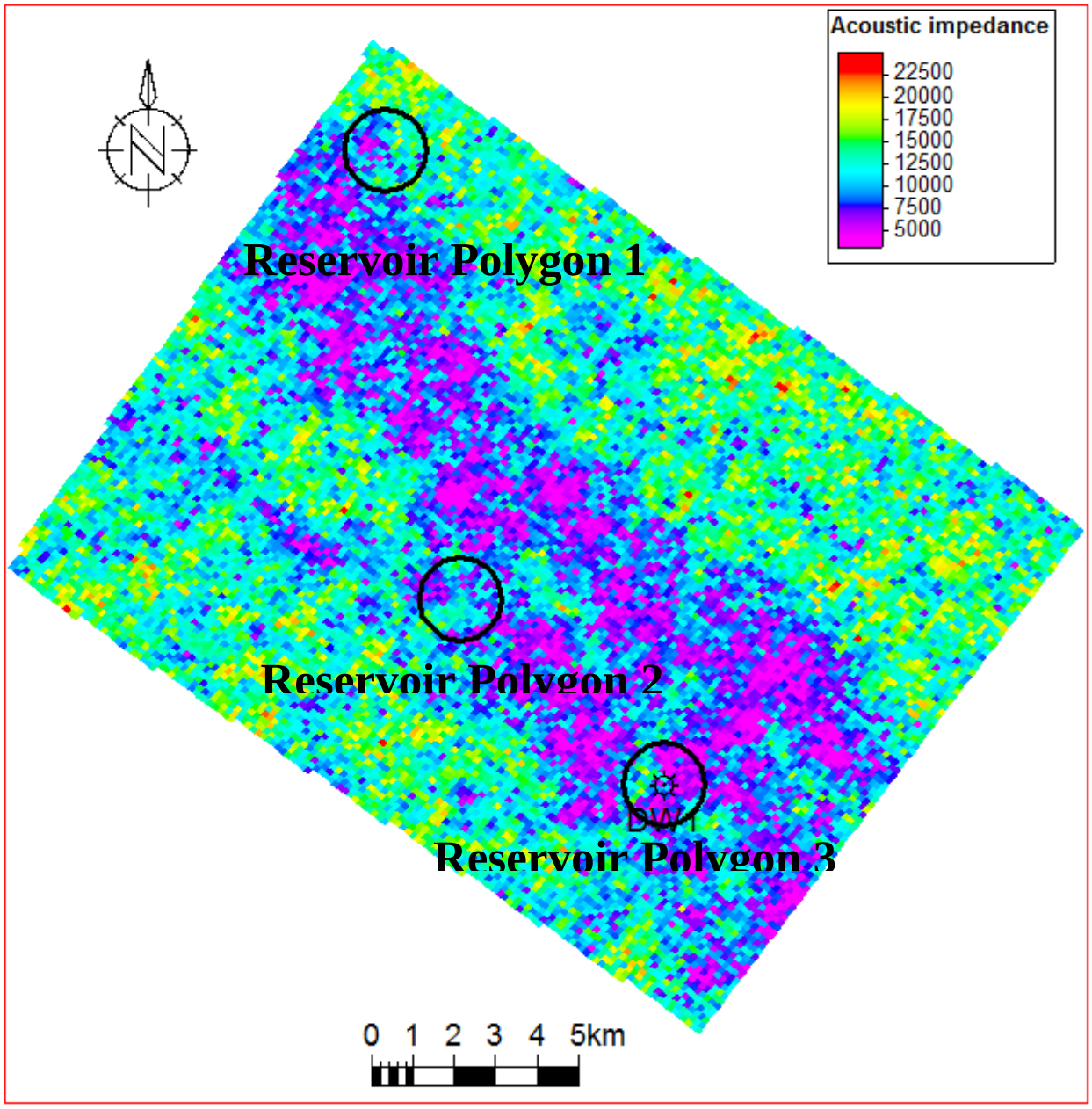

Figure 45: The seismic acoustic impedance cube

As seen in Figure 45 the seismic acoustic impedance responses shows a channel like structure with low impedance values (purple-blue), embedded in high acoustic impedance values shown in green-yellow-

red. The low acoustic impedance responses show a trend from SE to NW, while relatively high acoustic impedance response does not show any obvious structure.

Figure 46 explains the distribution of the probability of the reservoir facies, as a function of the acoustic impedance. It shows, a gradual decrease of the probability of the reservoir facies (yellow), with increasing acoustic impedance values, In Figure 46, which shows the probability distribution of non-reservoir facies (purple), the probability distribution of non-reservoir facies is increasing, whereas the acoustic impedance values increasing.

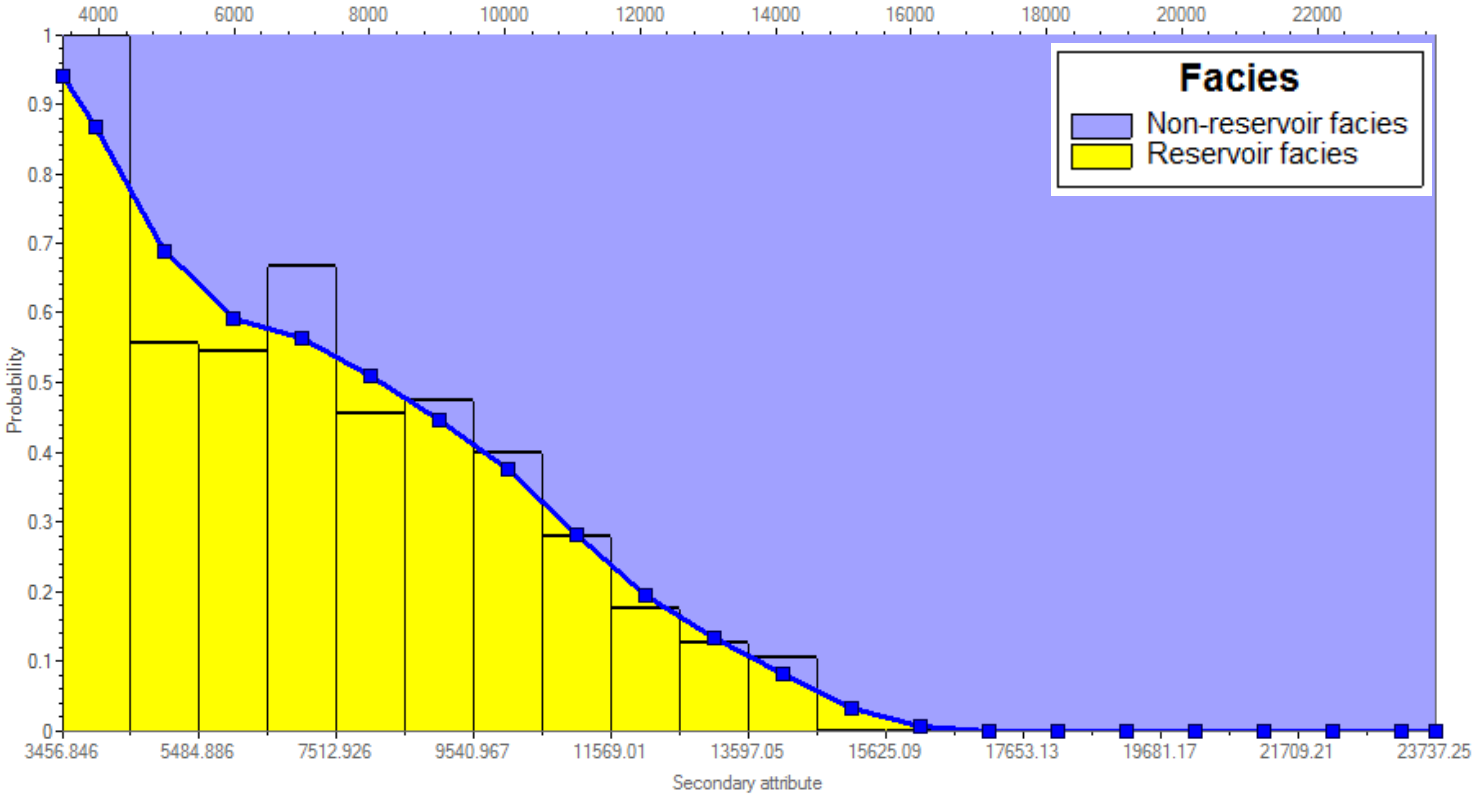

Figure 46: Reservoir facies probability distribution, according to acoustic impedance responses

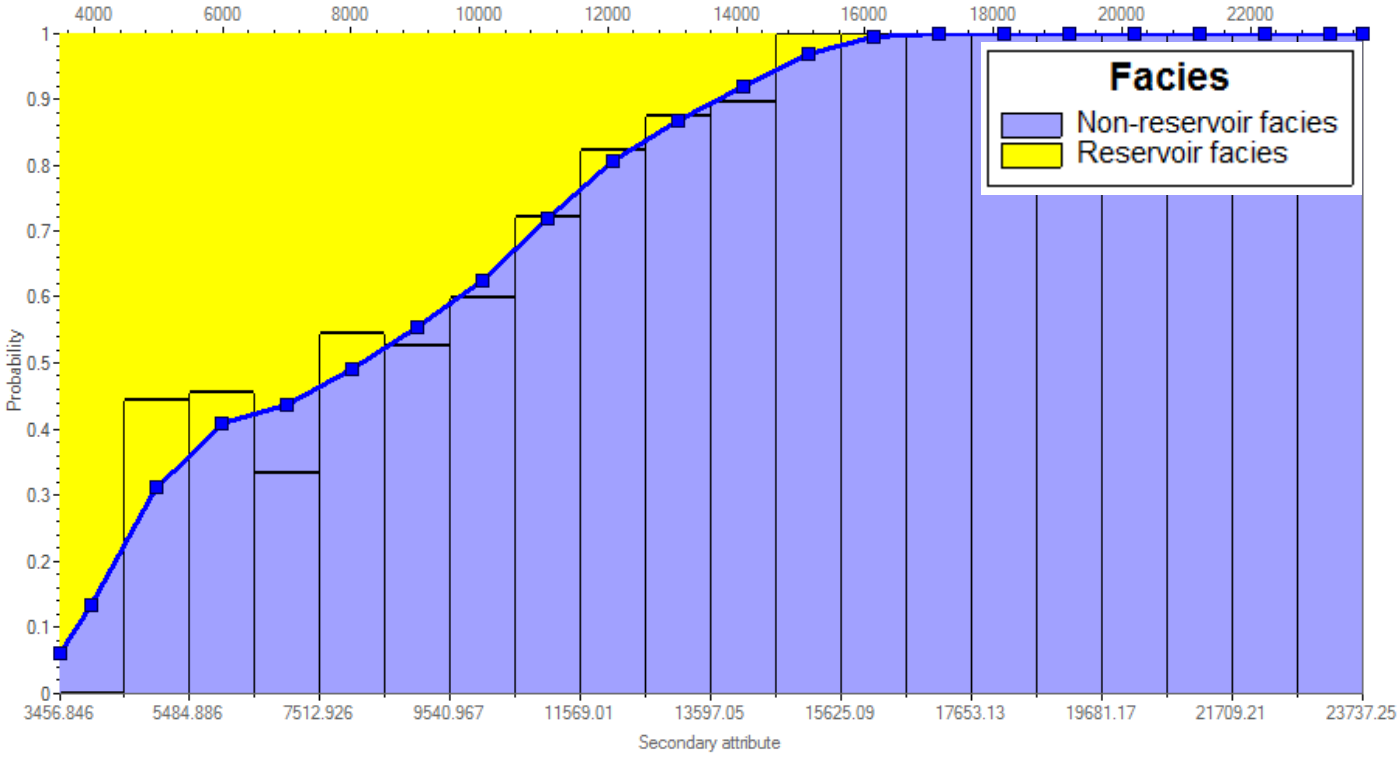

Figure 47: Non-Reservoir facies probability distribution, according to acoustic impedance responses

According to the reservoir and non-reservoir facies probability graphs, reservoir (sand) facies (Figure 48) and non-reservoir (shale) facies (Figure 49) probability acoustic impedance cubes are constructed.

Figure 48 shows the probability of reservoir facies, according to the acoustic impedance values. In this Figure, acoustic impedance values with high probability of reservoir facies are represented with yellow-green colors, therefore, it is clearly seen, that sand facies distribution at this time slice, have a SE-NW trend.

The probability of non-reservoir facies according to the acoustic impedance responses is represented on Figure 49. As the impedance time slice shows, high probability non-reservoir (shale) facies which are represented by yellow-orange color are distributed on the sides of the conceptual model

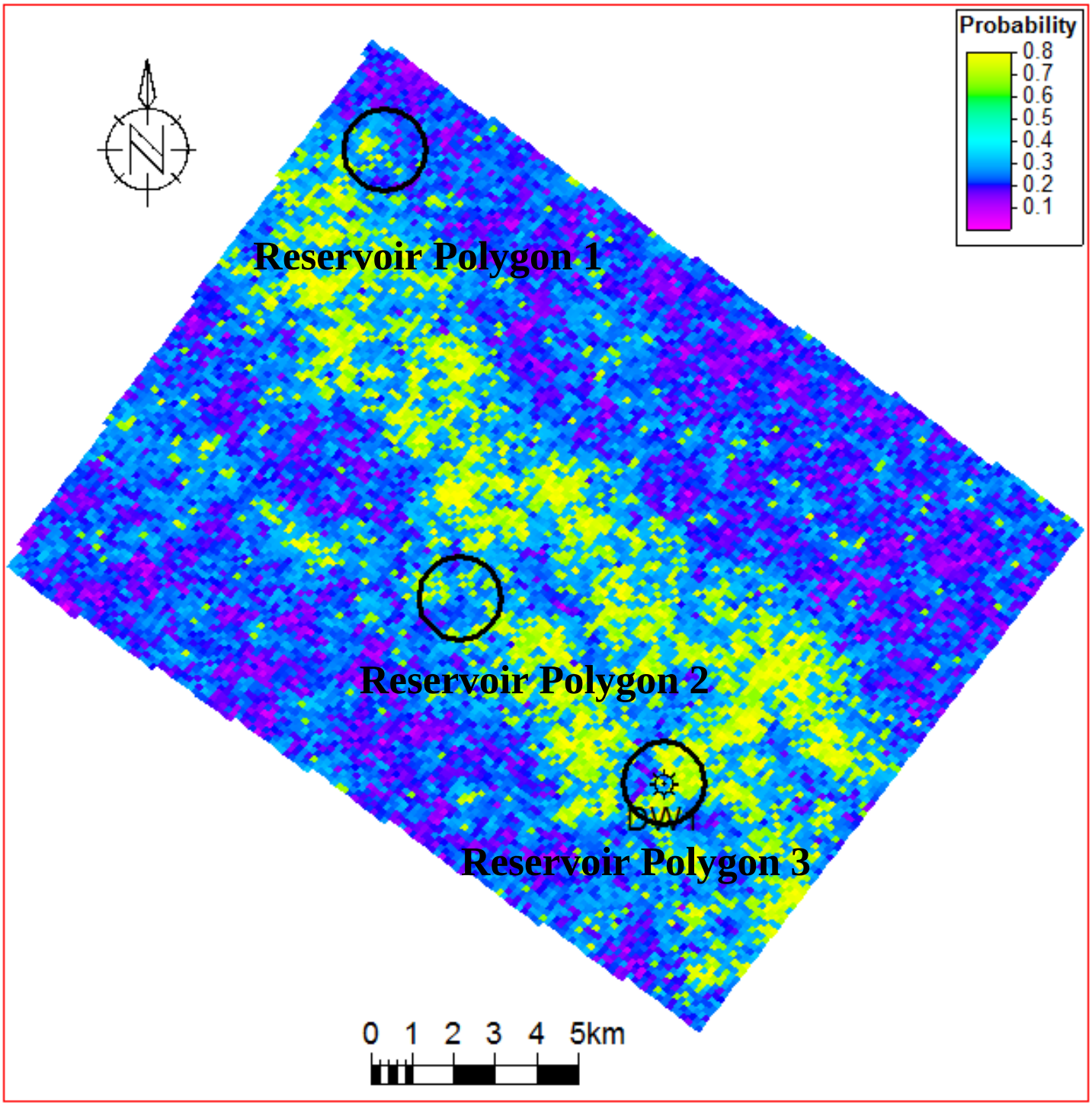

Figure 48: Reservoir (sand) facies probability cube

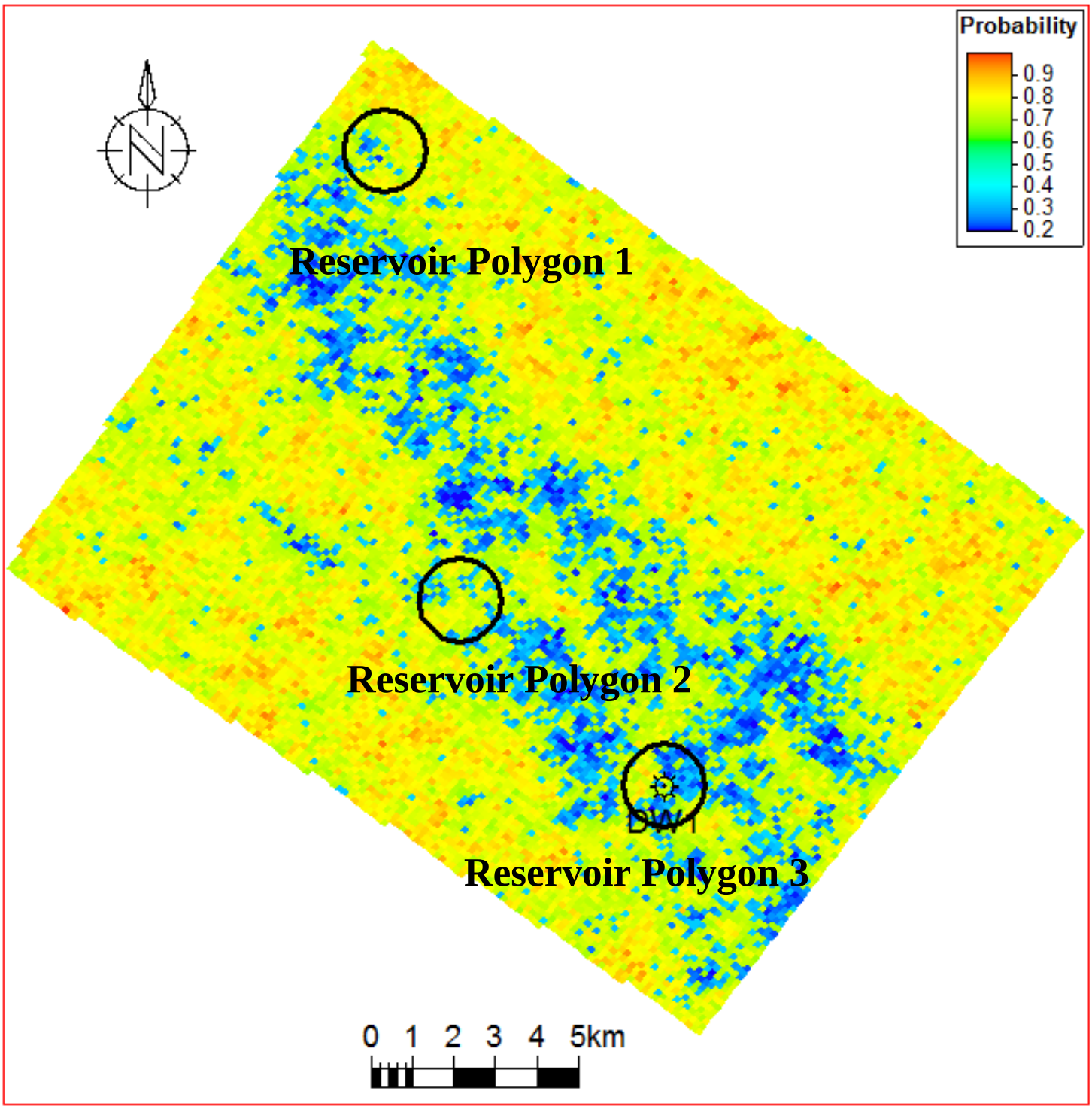

Figure 49: Non-reservoir (shale) facies probability cube

As shown in Figure 50a, the volume spread distributions for polygon 3 (around the well) with radius 500m, were plotted as a function of the horizontal variogram range. Color coded are the vertical anisotropy ranges: 1m, 10m and 50m. The probability cubes shown in figure 49 were used to guide the facies simulations. Figure 50b, represents the volume spread distributions, obtained using Sequential Indicator Simulation modeling method, and using the same modeling parameters, as in figure 50a but without the facies probability cubes derived from the acoustic impedance cube. The reservoir volume spread results for the Sequential Indicator Simulation guided by the seismic impedance cube are smaller compared to the results of Sequential Indicator Simulation modeling method that does not take the seismic impedance into account.

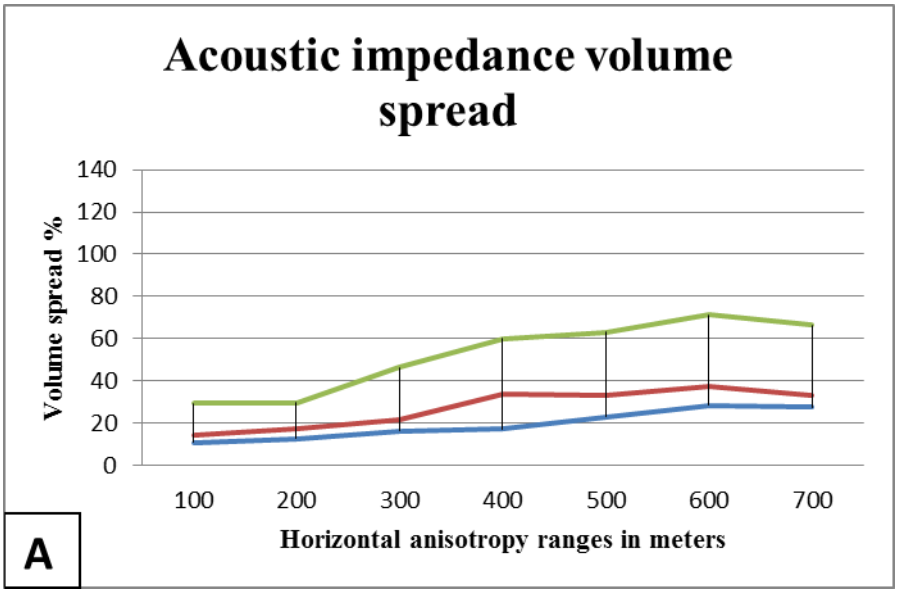

Figure 50: a) Reservoir volume spread distributions for Acoustic impedance in polygon 3 with radius 500m, using different vertical ranges.

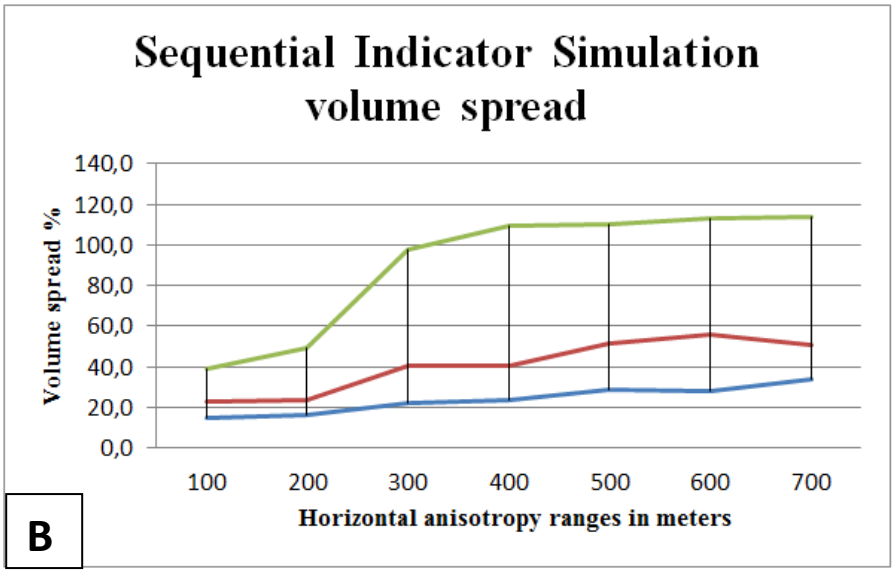

b) Reservoir volume spread distributions for Sequential Indicator Simulation in polygon 3 with radius 500m, using different vertical ranges

Figure 51a and Figure 51b, are comparing the reservoir volume spread results for reservoir polygon 3 and polygon 1, by using Sequential Indicator Simulation modeling method guided by the Acoustic impedance cube (blue function) and without the acoustic impedance cube (red function) . The reservoir volume spread function based on the Sequential Indicator Simulation method not guided by the acoustic impedance cube for Polygon 1, which is located away from the well DW 1, is higher than volume spread function for polygon 3. However for the Sequential Indicator Simulation guided by the Acoustic Impedance, the reservoir volume spread functions for Polygon 1 and Polygon 3 are very similar. In both cases, the reservoir volume spread distributions obtained by taking the Acoustic Impedance cube into account are smaller, comparing to volume spread distributions of the Sequential Indicator Simulation method without taking the acoustic impedance cube into account. A summary of the volume spread results are given in the Table 18 and Table 19:

(Acoustic Impedance) Polygon radius 500m		
Variogram ranges	100m	700m
Polygon 1	13 %	43 %
Polygon 3	14 %	33 %

Table 18: Volume spread based on Sequential Indicator Simulation guided by the Acoustic impedance volume for Polygon 1 and Polygon 3

(Sequential Indicator Simulation) Polygon radius 500m		
Variogram ranges	100m	700m
Polygon 1	24 %	81 %
Polygon 3	23 %	56 %

Table 19: Volume spread based on Sequential Indicator Simulation for Polygon 1 and Polygon 3

Figure 52a and Figure 52b show the comparison of the reservoir volume distribution for polygon 1 for both methods: by using Seismic acoustic impedance cube (Figure 52a) and Sequential Indicator Simulation method (Figure 52b). As it can be seen from the figures, the P50 value in the model with Seismic acoustic impedance shows is larger compared to P 50 value of Sequential Indicator Simulation. Therefore the reservoir volume distribution of the polygon with Seismic acoustic impedance is lower compared to Sequential Indicator Simulation.

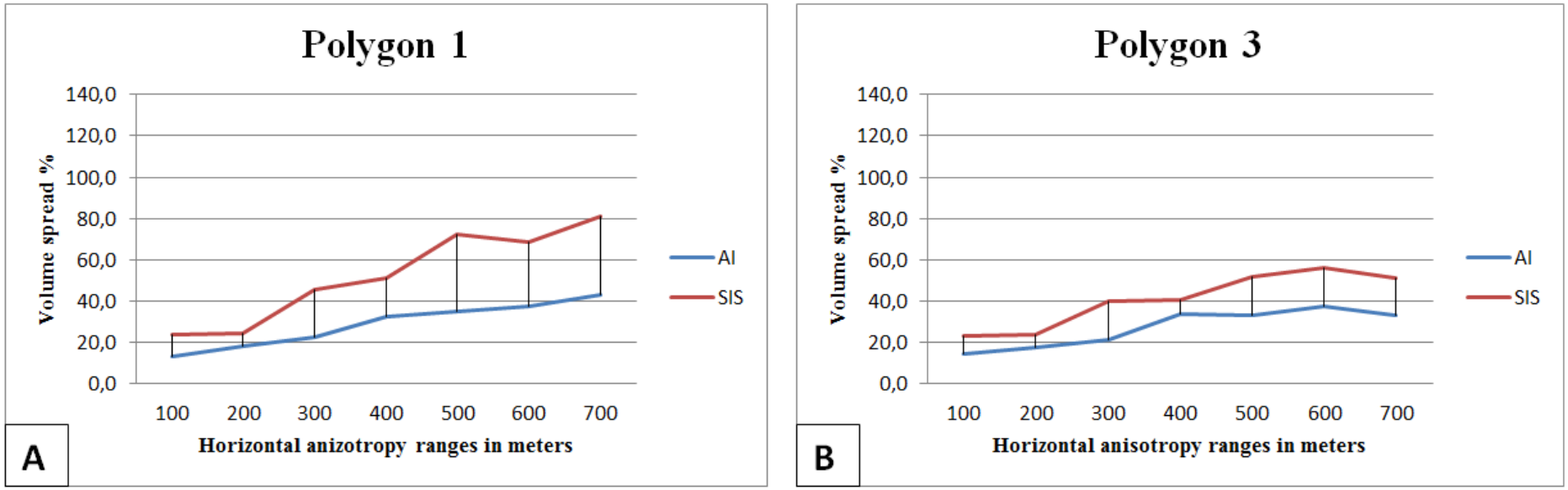

Figure 51: a) Reservoir volume spread distributions for polygon 1 with radius 500m using equal horizontal anisotropy ranges. b) Reservoir volume spread distributions for polygon 3 with radius 500m using equal horizontal anisotropy ranges.

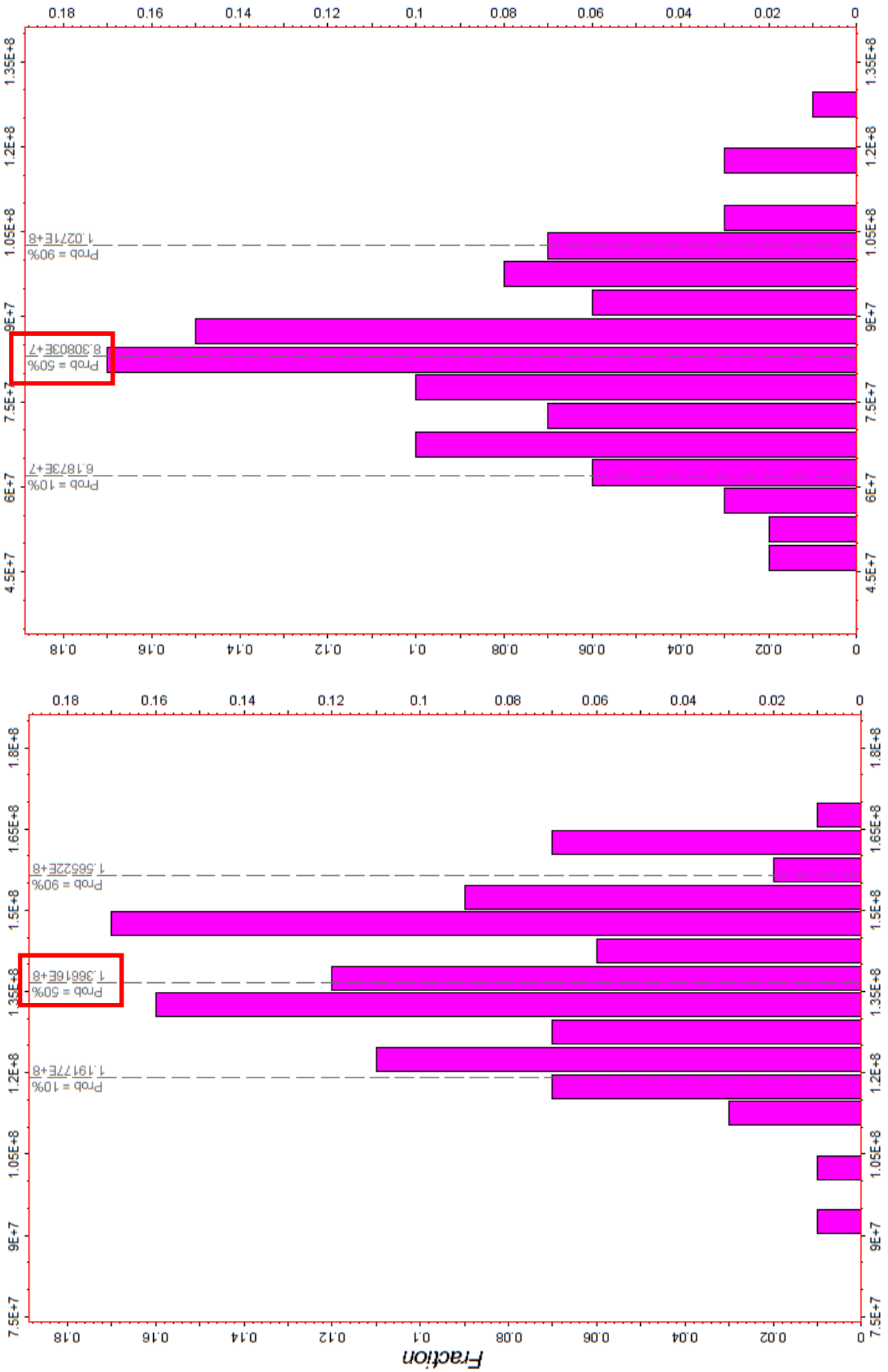

Figure 52: a) Reservoir volume distribution for polygon 1 with radius 500m, obtained using Seismic acoustic impedance cube. b) Reservoir volume distributions for polygon 1 with radius 500m using Sequential Indicator Simulation method.

Chapter 3 : DISCUSSION

This study is focusing on the influence of facies modeling parameters on the volume uncertainty of small reservoirs. It identifies the parameters that are most influential on the volume uncertainty and tries to show that the relationship between the reservoir size and the value of the parameters controlling the sand facies size are influencing the volume uncertainty to a large extend.

3.1 Sequential Indicator Simulation

As stated in the previous chapters, each modeling parameter has its own influence on reservoir volume spread. As the observations show, the rate of the influence differs from parameter to parameter. That basically means that some of the modeling parameters have higher influence on reservoir volume spread than others.

In Sequential Indicator Simulation modeling method, the parameters which are influencing the reservoir volume spread the most, are: Horizontal (Major range, Minor range) and Vertical ranges. This is clearly seen in Figure 36, where increasing variogram ranges are contributing to the considerable increase of the reservoir volume spread. Increasing variogram ranges, lead to larger reservoir facies patches and non-reservoir facies, which causes a higher reservoir volume spread.

3.2 Object Modeling

In Object Modeling, the most influential parameters are: Channel thickness and channel width. As it can be seen from the previous observations, Channel amplitude and wavelength don’t have such a significant impact on the reservoir volume, compared to channel thickness and channel width. Similar to Sequential Indicator Simulation modeling method, these two parameters control the reservoir facies patches and consequently have a major impact on reservoir volume accuracy.

Channel wavelength and channel amplitude variations, didn’t give any major differences in reservoir volume spread distributions. The reason is that these parameters do not control the size of the facies patches.

3.3 Reservoir size impact

One of the factors of importance for the reservoir volume distribution is the size of the reservoir. To simplify the analysis reservoirs defined by circular polygons with different radius of 500m and 1000m were used for the volumetrics. By comparing the reservoir volume spread graphs of these two polygons it becomes obvious that the uncertainty in the reservoirs with smaller radius is higher than in reservoirs with the larger radius. These results are coming from the higher probability of getting reservoir facies inside of the reservoir polygon with larger radius compared to the polygon with smaller radius.

3.4 Variation of the volume spread distribution in polygons with respect to the well

Reservoir polygon 3 is located around the well and therefore, the reservoir volume spread resulting from the variation of channel thickness and width is smaller, in comparison to reservoir polygon 1 and reservoir polygon 2. In other words the vicinity of a well reduces the reservoir volume uncertainty. The reason for this behavior is shown in Figure 53(below). The facies encountered at the well makes sure that a simulated channel is passing by the well in order to honor the sand facies at the channel. Consequently the polygon around the well will be crossed by a channel for every simulation (SEED number).

The situation is different for the other two polygons away from the well: In some models a channel passes through polygon 1 and polygon 2, in some cases it passes through polygon 2 without passing through polygon 1. The distribution of the channels is always changing with different Seed number. This causes the observed reservoir volume spread for polygon 1 and polygon 2.

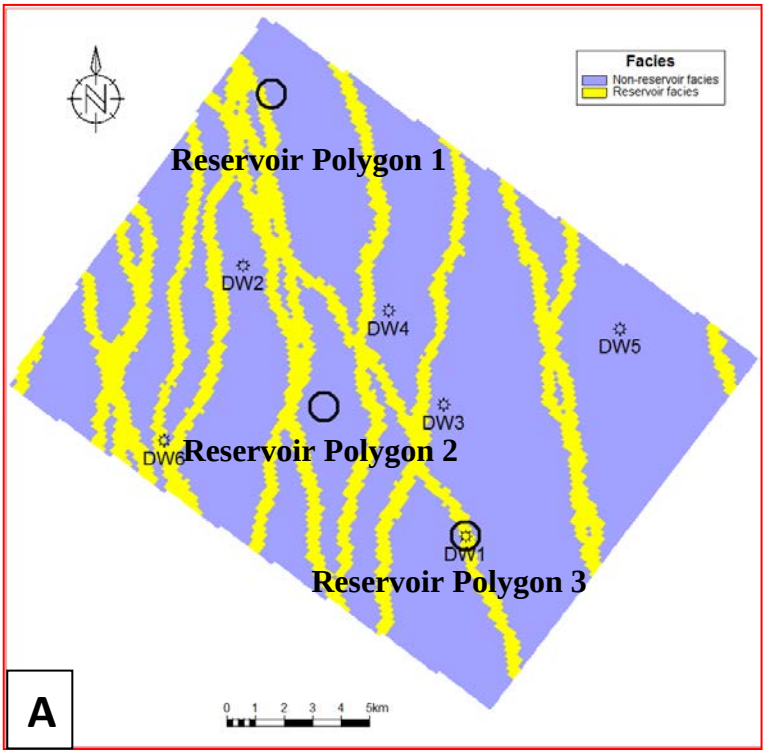

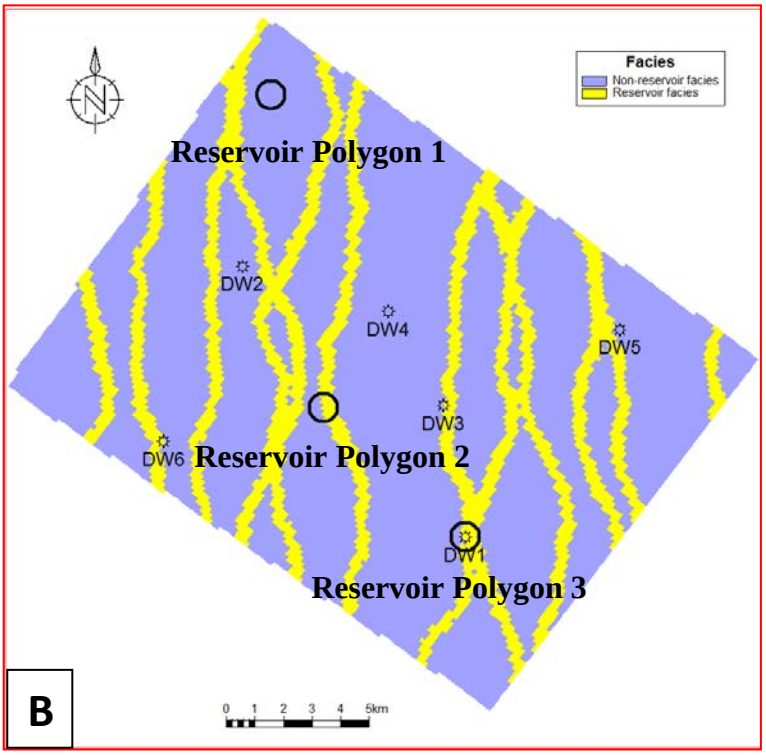

Figure 53: a) Channel distributions in Object modeling method. Seed number 10 b) Channel distributions in Object modeling. Seed number 50

3.5 Influence of Acoustic impedance cube on reservoir volume spread

The influence of the acoustic impedance cube on the reservoir volume spread was studied for the Sequential Indicator Simulation. The analysis is done for polygon 1 being far away from the well and polygon 3 which includes the well. Obviously the acoustic impedance cube has a reducing effect on reservoir volume spread compared to Sequential Indicator Simulation method without acoustic impedance as secondary input. . Note that the volume spread distributions for both polygons are quite similar. In addition it increases the P50 value of the volume for both polygons. The explanation for this observation is in Figure 54. The figure shows the average reservoir facies probability based on the acoustic impedance (54 A) and based on Sequential Indicator Simulation (54 B). Within the two polygons the reservoir facies probability shows higher values (ca 28%) compared to Sequential Indicator Simulation (ca 17%). This explains the difference in the P50 volumes for the two cases. For small reservoirs the reservoir volume uncertainty should decrease with increasing reservoir facies probability which is confirmed by the observation.

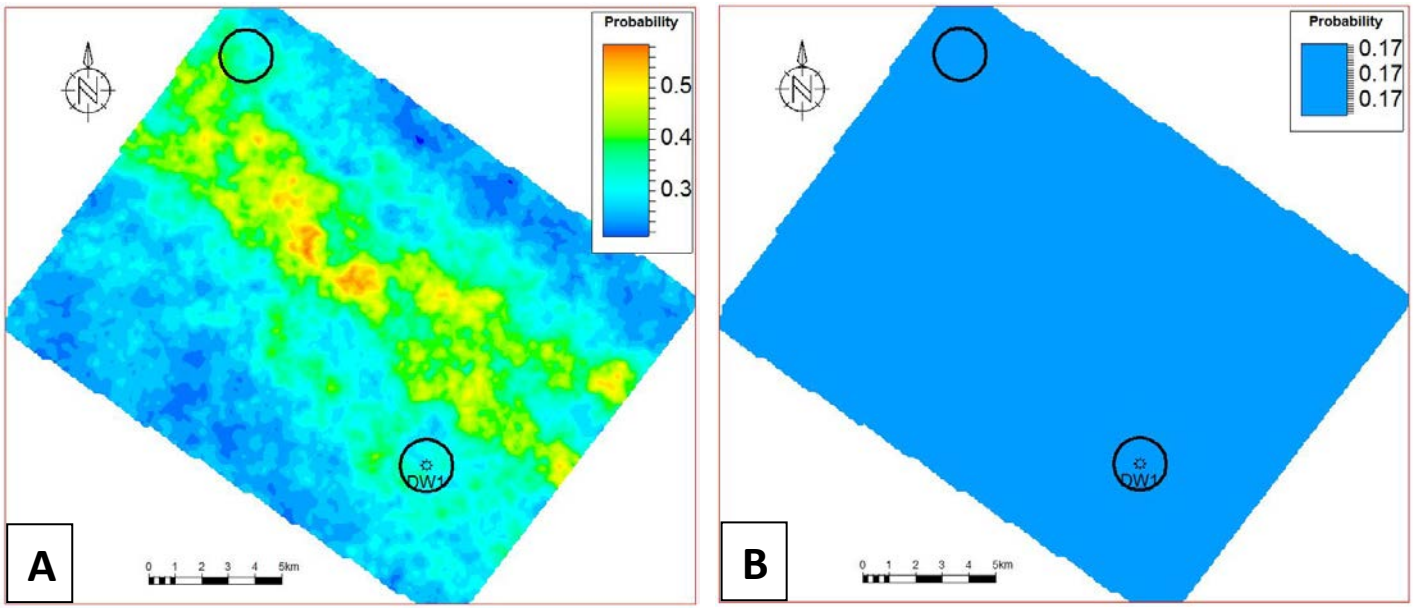

Figure 54: a) Sand probability of the model based on Acoustic impedance b) Sand probability of the model based on Sequential Indicator Simulation

3.6 Reservoir volume P50 stability, along with P10 and P90 values

The stability of P50 along with P10 and P90 in Object modeling method is shown in Figure 55. These graphs are created, based on P10, P50 and P90 values of the volume distributions of Object modeling. As can be seen, the P50 reservoir volume trend of three polygons is nearly horizontal, whereas the P10 has decreasing trend, and at the same time the P90 reservoir trend is increasing.

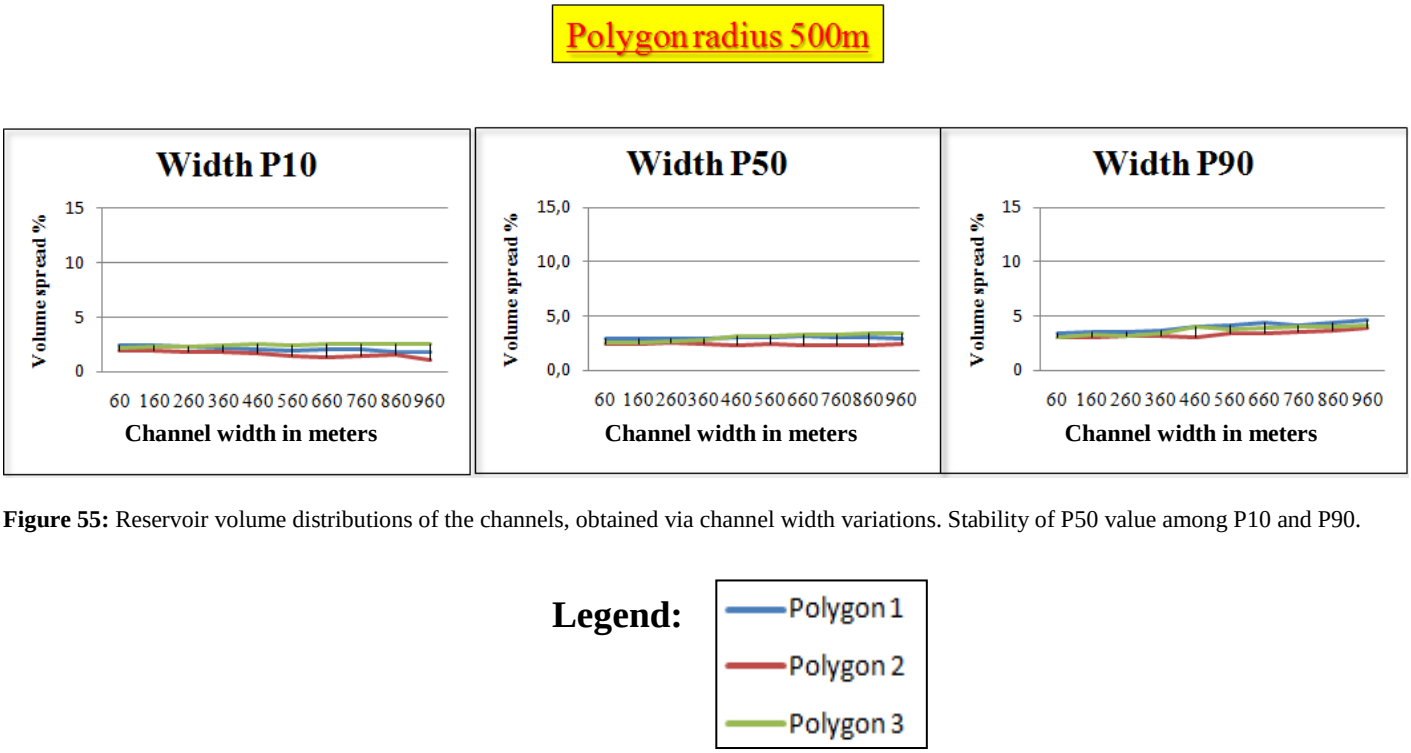

Figure 55: Reservoir volume distributions of the channels, obtained via channel width variations. Stability of P50 value among P10 and P90.

3.7 Volume spread analysis for Sequential Indicator Simulation and Object modeling methods

As the graphs are showing, in Object modeling and Sequential Indicator Simulation modeling methods, when the area of the investigation is getting closer to the well, a reduction in the reservoir volume spread is observed (Figure 56). The results obtained from Object Modelling, shows the nearly horizontal trend of stabilized volume spread for polygon 3. The volume spread is increasing with the variogram range for the other two polygons (Figure 57). To investigate smaller the lower reservoir

volume spread of Polygon 3 for Object Modeling method, compared to the volume spread coming from Sequential Indicator Simulation, it was decided to create, thickness maps for both methods.

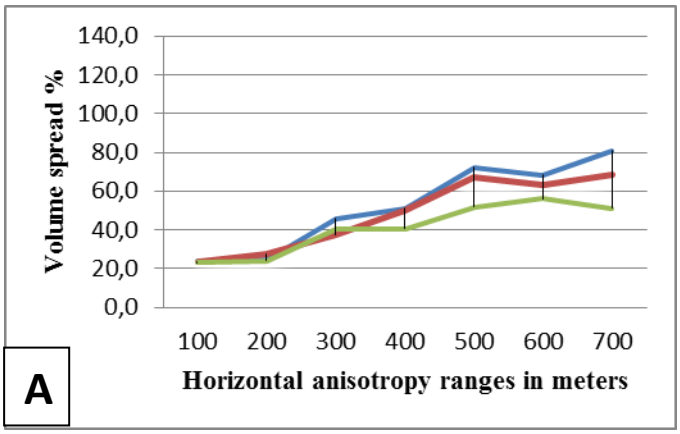

Figure 56: Sequential Indicator Simulation method. Reservoir volume spread distributions for different polygons with radius 500m. Vertical range is taken 10m.

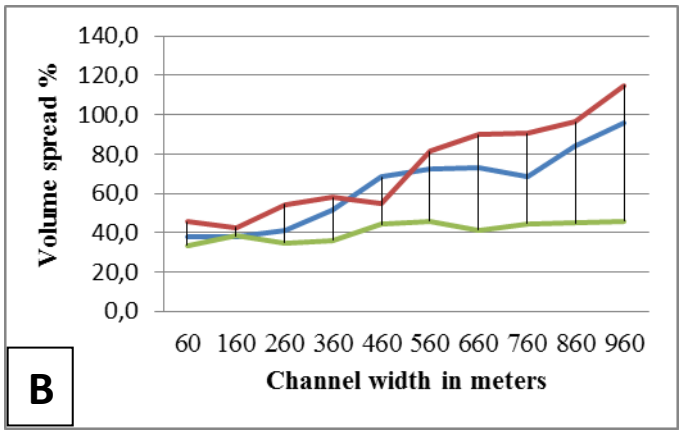

Figure 57: Object modeling method. Reservoir volume spread distributions for different polygons with radius 500m.

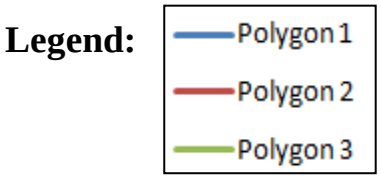

The thickness maps for Sequential Indicator Simulation modeling method show several areas of low sand thickness. It should be noted, that from simulation to simulation the positions of the high and low sand thickness patches is changing. This explains the large variations of the reservoir volume spread, also for the polygon around the well. Important: it can be assumed that the volume spread for the area of interest around the well is reduced in case of large horizontal variogram ranges (Figure 58).

The areas of high channel sand thickness are larger than the patches of sand based on Sequential Indicator Simulation. The upscaled sand facies at the well is making sure that a channel is always crossing the well for every simulation. Consequently the reservoir channel sand thickness in the vicinity of the well is similar for all simulations. Therefore, the reservoir volume spread for polygon 3 around the well is reduced comparing to the other reservoir polygons (Figure 59).

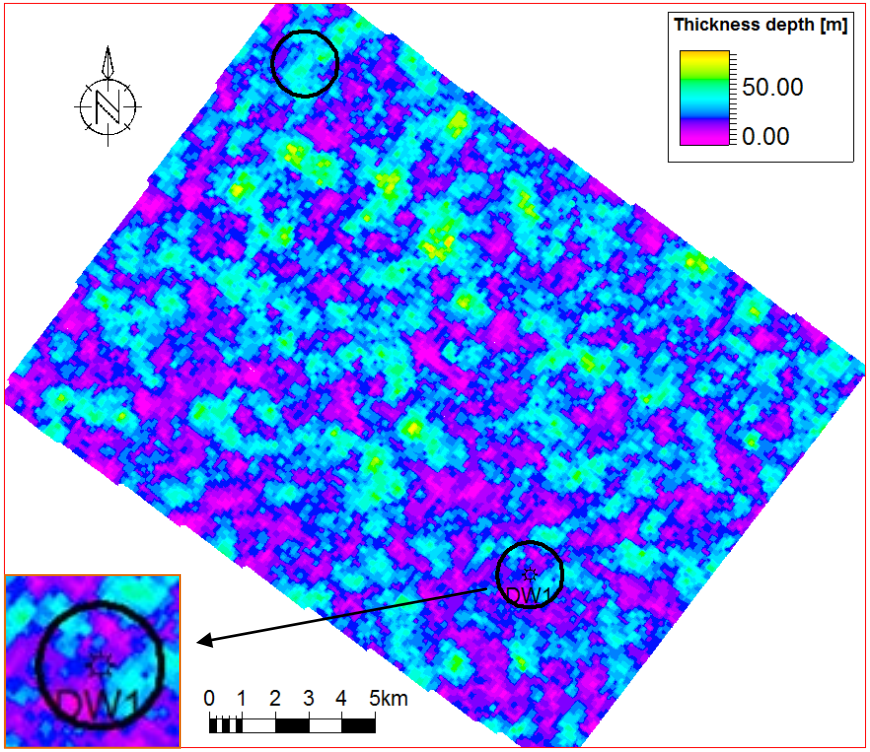

Figure 58: Reservoir facies (sand facies) thickness map for one Sequential Indicator Simulation. Major and Minor ranges are equal (700). Vertical range is 50

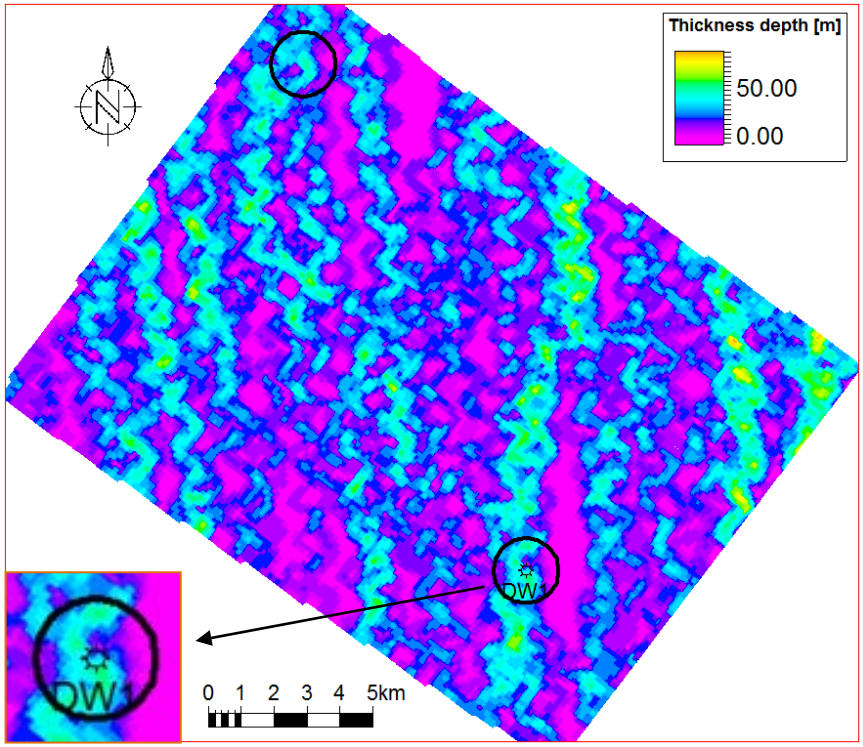

Figure 59: Reservoir facies (sand facies) thickness map for one Object Modelling method. Channel width is 960m.

Chapter 4 : CONCLUSIONS

The main conclusions of this research analysis of the influence of different modeling techniques on reservoir volume are:

- The parameters in Sequential Indicator Simulation modeling method, which are influencing the reservoir volume spread, are Horizontal and Vertical variogram ranges.
- The parameters in Object Modeling method, which are influencing significantly the reservoir volume spread, are channel thickness and channel width.
- Comparing the reservoir volume spread of the two modeling methods, shows that for indicator simulation the reservoir volume spread is reduced moderately from Polygon 1 to Polygon 3 (around the well) , However for Object modeling, the difference between the reservoir volume spread of Polygon 3 is much larger compared to Polygon 1 and Polygon 2
- The size of the reservoir polygon also plays an important role in the distribution of reservoir volume spread. The larger reservoir polygon, the smaller reservoir volume spread distribution appears to be.
- The reservoir volume spread increases with increasing distance of the polygon to the well. The Acoustic impedance cube has a noticeable impact on the reservoir volume spread. By using an Acoustic impedance cube for the facies simulation, the reservoir volume spread of the reservoir polygons, decreases comparing to Sequential Indicator Simulation without the impedance cube as secondary input

Each of the modeling methods, have advantages and disadvantages. The major advantages of Sequential Indicator Simulation method are:

- Possibility of building reservoir model with limited data
- Workflow running takes less time compared to Object modeling.
- There are only 3 influential parameters on the model and reservoir volume spread.

The possibility of creating accurate fluvial models is regarded as an advantage of Object modeling method.

Disadvantages of Object modeling method are:

- Workflow running time is more, comparing to Sequential Indicator Simulation method.
- The number of parameters, which are influencing the reservoir volume spread is higher, than for Sequential Indicator Simulation modeling
- There are four main parameters in Object Modeling method which are influencing the reservoir volume spread, the most. The main challenge in Object Modeling method is to get a proper estimation of the value range for these parameter

REFERENCES

Becquey, M., M. Lavergne, and C. Willm, 1979, Acoustic impedance logs computed from seismic traces: *Geophysics*, v. 44, p. 1485-1501.

Caers, J., 2005, Petroleum Geostatistics, *Society of Petroleum Engineers.*

Carlston, C. W., 1965, The relation of free meander geometry to stream discharge and its geomorphic implications: *American Journal of Science*, v. 263, p. 864-885.

Leeder, M. R., 1973, Fluviatile fining-upwards cycles and the magnitude of palaeo-channels: *Geological magazine*, v. v. 110, p. p. 265-276.

Leopold, L. B., and M. G. Wolman, 1960, River Meanders: *GSA Bulletin*, v. v. 71, p. p. 769-794.

Seifert, D., and J. L. Jensen, 1999, Using Sequential Indicator Simulation as a Tool in Reservoir Description: Issues and Uncertainties: *Mathematical Geology*, v. 31, p. 527-550.

Wonham, J. P., S. Jayr, R. Mougamba, and P. Chuilon, 2000, 3D sedimentary evolution of a canyon fill (Lower Miocene-age) from the Mandorove Formation, offshore Gabon: *Marine and Petroleum Geology*, v. 17, p. 175-197.